Journal of Colloid and Interface Science 652 (2023) 1308–1324

Contents lists available at ScienceDirect

Journal of Colloid And Interface Science

journal homepage: www.elsevier.com/locate/jcis

All natural mussel-inspired bioadhesives from soy proteins and plant derived polyphenols with marked water-resistance and favourable antibacterial profile for wound treatment applications

Rita Argenziano [a,b], Sara Viggiano [a], Rodolfo Esposito [a], Martina Schibeci [a], Rosa Gaglione [a], Rachele Castaldo [c], Luca Fusaro [d], Francesca Boccafoschi [d], Angela Arciello [a], Marina Della Greca [a], Gennaro Gentile [c], Pierfrancesco Cerruti [e], Gerardino D'Errico [a], Lucia Panzella [a], Alessandra Napolitano [a,*]

[a] Department of Chemical Sciences, University of Naples "Federico II", Naples, Italy
[b] Department of Agricultural Sciences, University of Naples "Federico II", Naples, Italy
[c] Institute for Polymers, Composites and Biomaterials - CNR, Pozzuoli (NA), Italy
[d] Department of Health Sciences, University of Piemonte Orientale, Italy
[e] Institute for Polymers, Composites and Biomaterials (IPCB-CNR), CNR, Pozzuoli (Na), Italy

GRAPHICAL ABSTRACT

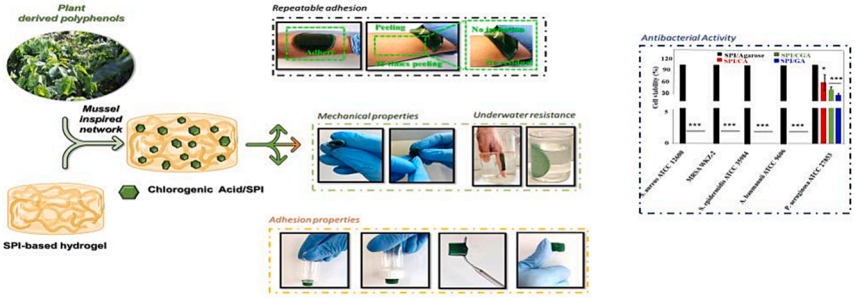

ARTICLE INFO

Keywords:
Polyphenols
Soy proteins
Hydrogel
Bioadhesives
Surgical glues
Underwater resistance
Antibacterial activity

ABSTRACT

Hypothesis: Implementation of tissue adhesives from natural sources endowed with good mechanical properties and underwater resistance still represents a challenging research goal. Inspired by the extraordinary wet adhesion properties of mussel byssus proteins resulting from interaction of catechol and amino residues, hydrogels from soy protein isolate (SPI) and selected polyphenols i.e. caffeic acid (CA), chlorogenic acid (CGA) and gallic acid (GA) under mild aerial oxidative conditions were prepared.

Abbreviations: SPI, soy protein isolate; CGA, chlorogenic acid; GA, gallic acid; CA, caffeic acid; DOPA, 3,4-dihydoxyphenylalanine; DTNB, 5,5′-dithio-bis(2-nitrobenzoic acid); EDTA, ethylenediaminetetraacetic acid; SDS, sodium dodecyl sulfate; OPA, *o*-phthalaldehyde; HaCaT, human keratinocyte; HDF, human dermal fibroblasts; EPR, electron paramagnetic resonance; ATR FT-IR, attenuated total reflection infrared; SEM, scanning electron microscopy.

* Corresponding author.
E-mail address: alesnapo@unina.it (A. Napolitano).

https://doi.org/10.1016/j.jcis.2023.08.170
Received 16 June 2023; Received in revised form 6 August 2023; Accepted 26 August 2023
Available online 28 August 2023

Wound healing properties
Water-vapour permeability

Experiments: The hydrogels were subjected to chemical assays, ATR FT-IR and EPR spectroscopy, rheological and morphological SEM analysis. Mechanical tests were carried out on hydrogels prepared by inclusion of agarose. Biological tests included evaluation of the antibacterial and wound healing activity, and hemocompatibility.
Findings: The decrease of free NH_2 and SH groups of SPI, the EPR features, the good cohesive strength and excellent underwater resistance (15 days for SPI/GA) under conditions relevant to their use as surgical glues indicated an efficient interaction of the polyphenols with the protein in the hydrogels. The polyphenols greatly also improved the mechanical properties of the SPI/ agarose/polyphenols hydrogels. These latter proved biocompatible, hemocompatible, not harmful to skin, displayed durable adhesiveness and good water-vapour permeability. Excellent antibacterial properties and in some cases (SPI/CGA) a favourable wound healing activity on dermal fibroblasts was obtained.

1. Introduction

The quest for adhesives for soft tissues repair is nowadays very actively pursued and indeed many different solutions have been developed in the literature, including mainly hydrogels. Among the several requirements that should be met by these materials is biocompatibility, coupled possibly with antibacterial activity to increase their potential in wound healing treatment. Additionally, tissue adhesives should be endowed with good to excellent mechanical properties under physiologically relevant conditions, and particularly under-water resistance, this latter remaining a major challenge in the design of these materials.

In this regard the mechanisms of adhesion of the marine organisms represent an unvaluable source of inspiration. One of the most widely exploited is that of mussel byssus foot proteins whose extraordinary wet adhesion properties result from interaction of the catechol system of the abundant 3,4-dihydoxyphenylalanine (DOPA) residues with lysine amino groups giving rise to cross-linked networks. Accordingly, enormous efforts have been devoted to the development of synthetic mussel-inspired materials with water-resistant adhesion and cohesion properties based on covalent and noncovalent interactions including oxidative cross-linking, electrostatic interaction, metal–catechol coordination, hydrogen bonding, hydrophobic interactions and π–π/cation–π interactions [1]. These are obtained by modifying polymer systems with DOPA or using its analogue dopamine that combines the catechol and amino functionality [2–6].

Cross-linking of Al^{3+}-coordinated alginate-dopamine chains with acrylamide-acrylic acid polymers resulted in hydrogels endowed with good mechanical properties in which the catechol functionality of dopamine ensured robust fibroblast cell adhesion [7]. Nanocomposite hydrogels incorporating dopamine catechol moieties conjugated to natural anionic poly(γ-glutamic acid) and cross-linked through horseradish peroxidase/hydrogen peroxide oxidation, with an additional physical cross-linking with a synthetic bioactive nanosilica, showed strong adhesiveness to various tissue layers and demonstrated excellent haemostatic properties [8]. Simple inclusion of DOPA resulted in fortification of porous and erodible chitosan-based adhesive films that may be used for fabrication of photochemical tissue bonding systems by use of light and a photosensitiser to promote tissue adhesion [9].

Concerns of potential neurological effects entailed by the use of dopamine in the mussel-inspired strategy was overcome by use of alternative phenolic compounds. Oxidative coupling of tannic acid with nucleophilic residues of animal gelatin allowed access to low-cost and readily scalable water-resistant plant-inspired bioadhesives [10]. Similarly, a plant catechol-based adhesive was prepared relying on the redox abilities of lignin nanoparticles giving rise to a pectin-polyacrylic acid hydrogel network by initiating radical polymerization of acrylic acid [11,12].

In addition to polysaccharides and synthetic polymers, proteins from easily accessible sources have also been explored for preparation of bioadhesives [13]. Of particular relevance in this connection are soy proteins isolate (SPI), the main industrial waste in soybean processing, that appear ideal candidate for implementation of environmentally friendly biomass-based adhesives since they are cost-effective, easy to handle, and have been considered as alternative aldehyde-free materials also in wood industry [14,15]. In addition, these proteins are rich in amino groups with lysine content up to 6% [14]. Notwithstanding that, SPI based hydrogels have very scanty applications due to their weak resistance under water, cumbersome gelation process and poor mechanical properties. Chemical cross-linking modification is the most potent way to enhance performance of soy proteins, using either synthetic or natural compounds, that have been in many cases covalently linked to the protein scaffold [16–21]. Plant extract enriched with phenolic or polyphenolic compounds exhibited synergistic effect in inducing the gelation of biopolymers [22–24].

Cross-linking hinging on oxidation chemistry of polyphenols has also been exploited to get high performance materials using tannic acid [25], modified tannins [26], lignins [27] or other phenolic polymers [28].

Yet, exploitation of SPI as starting material for preparation of hydrogels with suitable properties for tissue repair has been so far scarcely explored.

In this work we report preparation of hydrogels from SPI and polyphenols of natural origin under mild aerial oxidative conditions. The underlying chemistry was explored by chemical assays, attenuated total reflection infrared (ATR FT-IR) and electron paramagnetic resonance (EPR) spectroscopies, while the morphology was investigated by scanning electron microscopy (SEM) analysis. Integration of polyphenols compounds in the SPI afforded glues exhibiting a noticeable underwater resistance when applied to both plywoods and animal tissues cuttings. To expand the potential of these materials to wound dressing applications, hydrogels from agarose/SPI were prepared and reacted with the selected polyphenols under oxidative conditions. These materials to which the polyphenols conferred reduced tensile strength and increased ductility showed contact-active antibacterial activity particularly against gram positive strains, good cytocompatibility toward dermal fibroblasts and keratinocytes, hemocompatibility and in some cases induced wound healing repair as assessed by the scratch test using relevant cell cultures.

2. Experimental section

2.1. Materials

Soy protein isolate (SPI) (99%) was purchased from commercial sources (MyProtein) and used without further purification. Caffeic acid (CA), chlorogenic acid (CGA), gallic acid (GA), agarose (analytical nucleic acid electrophoresis grade) and all other reagents indicated in the following paragraphs were purchased from Sigma-Aldrich and used without further purification. Deionized water was used for all experiments. Wood specimen from pine were obtained from a carpenter shop. Chicken tissues (skin and muscle) were freshly obtained from a local butcher and stored at 4 °C until use, typically within 1–2 days.

2.2. Preparation of the SPI/polyphenols glues

SPI (1 g) was dissolved in water (10 mL) and kept at 85 °C for 1 h in a thermostatic bath to induce denaturation. The proper polyphenol was

then added to a final concentration of 28 mM. The resulting solution was brought to pH 9 by addition of 0.1 M NaOH, taken to 50 °C and left under stirring in air for 2 h. The resulting material was centrifuged at 7000 rpm, at 4 °C, over 10 min to remove excess water and then used for the experiments described infra. When required the materials were lyophilized.

2.3. Preparation of the SPI/agarose/polyphenols hydrogels

Denatured SPI (10% w/w) obtained as described above was added to a 2% w/w solution of agarose in water at 2:1 v/v and taken at 70 °C for 15 min, then poured in a Petri dish and allowed to cool at room temperature for 1 h. The resulting hydrogel was dipped in a 10 mM solution of the polyphenol in 0.05 M phosphate buffer at pH 9 in air. After 2 h the hydrogel was washed with water (3 × 10 mL). The hydrogels were air dried and then rehydrated before use by dipping in water in a Petri dish.

2.4. Determination of the NH_2 and SH content

2.4.1. Sulfhydryl groups

The sulfhydryl content of SPI/polyphenols glues was determined using the Ellman's reagent according to a protocol previously described [29]. Ellman's reagent was prepared by dissolving 5,5′-dithio-bis(2-nitrobenzoic acid) (DTNB) (4 mg) in 1 mL of Tris-glycine buffer (0.086 M Tris, 0.09 M glycine and 4 mM ethylenediaminetetraacetic acid (EDTA), pH 8.0). The powder from lyophilized SPI/polyphenols glues was dissolved in Tris-glycine buffer to a concentration of 3 mg/mL and mixed with 50 μL of Ellman's reagent. The mixed solution was left under stirring at room temperature for 1 h. A sample containing only denatured SPI was subjected to the same treatment and used as reference of the total SH groups. The absorbance at 412 nm was recorded on a Jasco V-730 spectrophotometer and the value corrected for the contribution of each SPI/polyphenol material at the concentration used (determined in the absence of Ellman's reagent). Data were expressed as the percentage of reacted SH groups in SPI/polyphenols with respect to those of the pure SPI. To determine the levels of free SH groups in the denatured SPI a calibration curve was built up using a glutathione solution at concentrations in the range 0.002–0.01 mg/mL (Figure S1 a).

2.4.2. Amino groups

The contents of free amino groups in the sample were determined using a slightly modified version of the *o*-phthalaldehyde (OPA) method applied to soy proteins [29]. OPA (40 mg) dissolved in methanol (1 mL), 20% (w/v) sodium dodecyl sulfate (SDS) solution (2.5 mL), 0.1 M borax solution (25 mL) and β-mercaptoethanol (100 μL) were combined. Finally, the OPA reagent was prepared by adding distilled water to the above solution to bring the total volume up to 50 mL in a volumetric flask. The samples were added to the OPA reagent to a final concentration of 0.18 mg/mL. After the mixture was thoroughly mixed and the reaction was allowed to proceed at 35 °C for 2 min, the absorbance of the sample was measured at 340 nm on a Jasco V-730 spectrophotometer. At each concentration used, the contribution of the sample to the absorbance at 340 nm (determined in the absence of the OPA reagent) was subtracted. Data were expressed as the percentage of reacted NH_2 groups in SPI/polyphenols with respect to those of the pure SPI. A calibration curve was built up using alpha BOC L-lysine at concentrations in the range 3–9 μg/mL (Figure S1 b).

2.5. ATR FT-IR measurements

ATR FT-IR spectra of the SPI/polyphenols glues as lyophilized powders were recorded by means of a Perkin Elmer Spectrum 100 spectrophotometer (USA), equipped with a Universal ATR diamond crystal sampling accessory. Spectra were recorded as an average of 16 scans, with a resolution of 4 cm^{-1}.

2.6. EPR measurements

A X-band spectrometer was used to conduct EPR measurements (Bruker, Rheinstetten, Germany). The samples were placed in flame-sealed glass capillaries that were coaxially collocated into a typical 4 mm quartz sample tube. Spectra were recorded at room temperature. The instrument parameters were as follows: modulation frequency: 100.00 kHz; modulation amplitude: 1.0 G; receiver gain: 60 dB; sweep width: 100 G; time constant: 10.24 ms; conversion time: 20.48 ms. In preliminary tests, microwave power was steadily increased from 0.001 to 128 mW in order to achieve power saturation. In order to prevent microwave saturation of the resonance absorption curve, single spectra were then obtained at a microwave power optimized for each sample. To increase the signal-to-noise ratio, several scans, around 128, were accumulated. A Mn^{2+}-doped MgO internal standard was used to measure the g value and the spin density. The broadness of each spectrum was calculated as the difference in gauss (G) between the detected signal's maximum and minimum (DB).

2.7. Morphological properties

Morphological analysis of the SPI/polyphenols glues was performed by scanning electron microscopy (SEM) using a FEI Quanta 200 FEG SEM in high vacuum mode. Before SEM observations, samples were mounted onto SEM stubs by means of carbon adhesive disks and sputter coated with a 5–10 nm thick Au-Pd layer. All the samples were observed at 10 kV acceleration voltage using a secondary electron detector.

2.8. Mechanical properties

2.8.1. Adhesive strength

Wood specimen from soft wood (pine) (30 × 20 × 50 mm thickness, width, and length) were used [30]. The SPI or SPI/polyphenol glues, prepared as described under paragraph 2.2, was weighted, and brushed on a 2 × 2 cm area of each piece (approx. protein concentration 1.80 mg/cm^2). The pieces were allowed to stand at room temperature for 5 min, assembled by hand and then pressed together with a clamp for 24 h. Shear strength of wood specimens was determined by using an Instron testing machine (model 4505) operated at a crosshead speed of 25 mm/min. The force (N) required to break the glued wood specimen was recorded. The failure stress of the adhesive was determined by measuring the lap shear strength, which corresponds to the force (N) required to tear apart the wood joints divided by the bonding area (in these experiments 4.0 cm^2). All the adhesive strength data reported are means of six replications. Prior to measurement the specimens were equilibrated for 48 h at 25 °C and 50% relative humidity (RH). For water resistance test the wood specimen were soaked in deionized water at room temperature and periodically checked.

2.8.2. Adhesion tests on animal tissues and underwater resistance

For tests on chicken skin a protocol previously described was adopted [31]. In brief, the fat layer below the skin was removed using a scalpel and the tissue was cut into pieces of approx. 15 × 20 mm, washed gently with hand soap once, rinsed with tap water, immersed in ethanol for 2 min and again rinsed with tap water. Skin samples prepared this way were kept immersed into 10 mM HEPES buffer at pH 7.5 for 30 min before their use for the adhesion tests. The SPI or SPI/polyphenols glues was deposited on the skin on a 2 × 2 cm area.

For the experiments using chicken breast muscle, slices of approx 5 × 3 mm were cut by a knife and then immersed in HEPES buffer as above, washed with deionized water and gently wiped onto a tissue paper to blot the excess of liquid. The SPI or SPI/polyphenols glues were subjected to a curing treatment by leaving them in air over 6 h, after which time they were applied on the slices. For the water resistance test skin samples were soaked in PBS at room temperature and periodically checked.

2.8.3. Rheological characterization

Rheological data of the SPI/polyphenols glues were collected using a HAAKE Rheo Stress 6000 (Thermo Scientific) rotational rheometer equipped with a parallel plate geometry, 20 mm plate diameter, and 2.0 mm gap, at 30 °C. Frequency sweep tests were performed at 2% strain, over a frequency range of 0.1–100 rad s^{-1}.

In order to evaluate self-healing properties of the hydrogels, time sweep tests were carried out at 1 rad s^{-1} and alternating 60-second segments at 1% and 100% strain.

Compressive stress–strain tests on the hydrogels were performed using the same equipment, with a loading–unloading strain rate of 0.6 mm/min, and a strain level up to ≈15% of the original plate gap. The loading step was followed by a 120-s stress relaxation segment, at the end of which the unloading step started.

2.8.4. Tensile tests

Tensile tests were performed on the SPI/agarose/polyphenols hydrogels conditioned for 3 days at 25 °C and 50% RH, using an Instron model 5564 dynamometer equipped with a 1 kN load cell, at 23 ± 2 °C, 45 ± 5% RH, with a 5 mm min^{-1} clamp separation rate. Four dog bone shaped specimens (50 mm overall length, 28 mm distance between the wide parallel sections, 4 mm width) were tested for each formulation.

2.9. Water vapor permeability (WVP) tests

WVP measurements of the SPI/polyphenol hydrogel were performed according to ASTM E96 standard method. Air dried hydrogels with exposed area of 2.83 cm^2 were sealed over a circular opening of aluminum permeation cells filled with distilled water. The cells were kept in an environmental chamber at 25 °C under 50% RH. After the system reached steady state conditions, the weight change of the cell was measured every 24 h. Air dried SPI/agarose/polyphenols hydrogels were tested three times to confirm repeatability of measurements (Figure S2).

The weight loss of hydrogels was plotted with respect to time, and the linear least-square method was used for the calculation of the parameters given by Equation:

$$WVP = L \times WVTR/\Delta P$$

where WVTR is the water vapor transmission rate of air-dried SPI/agarose/polyphenols hydrogels with (g s/m^2), L is average thickness of the hydrogels (m), ΔP is the difference in water vapor pressure between the two exposed sides of the hydrogels (Pa).

2.10. Cytocompatibility

Immortalized human keratinocytes (HaCaT) and human dermal fibroblasts (HDF) were cultured at 37 °C in a humidified atmosphere containing 5% CO_2 in high-glucose Dulbecco's modified Eagle's medium (DMEM) with 10% fetal bovine serum (FBS), 1% antibiotics (Pen/strep), and 1% L-glutamine. 24 h before treatment, cells were seeded on 96-well plates at a density 3×10^3 cells/well. The compounds (agarose (0.625 mg/mL) or agarose as above/0.875 mg/ml SPI or agarose/SPI as above/0.0875 mg/ml CGA/0.005 mg/ml CA or GA) were then added, and the mixture was incubated for 24 and 72 h. Following treatments, MTT assays were performed replacing the cell culture supernatants with 0.5 mg/mL MTT reagent dissolved in DMEM medium without red phenol (100 μL/well).After being incubated for 4 h at 37 °C, the resulting insoluble formazan salts were dissolved in 0.01 M HCl in anhydrous isopropanol, and determined by measuring the absorbance at 570 nm with an automatic plate reader spectrophotometer (Synergy H4 Hybrid Microplate Reader, BioTek Instruments, Inc., Winooski, VT). The percentage values in comparison to the control, untreated cells were used to express the cell viability. To perform Trypan blue exclusion test, cells were seeded on 96-well plates at a density 3×10^3 cells/well and cultured for 24 h as previously described to allow cell adhesion. Then, the culture medium was removed and replaced culture medium containing agarose (0.625 mg/mL) or agarose as above/0.875 mg/ml SPI or agarose/SPI as above/0.0875 mg/ml CGA/0.005 mg/ml CA or GA). Cells were incubated for 72 h at 37 °C prior to be treated with Trypsin (Trypsin-EDTA 1X in PBS w/o Calcium, w/o Magnesium, w/o Phenol Red) and stained with 0.5% Trypan Blue for 3 min. Blue (dead) and white (live) cells were then counted by using coverslip-microscope slides with grids. Experiments were performed in duplicate with triplicate determinations. The percentage of living cells was estimated as follow:

$$Cell\ viability(\%) = \frac{Number\ of\ living\ cells}{Number\ of\ total\ cells} * 100$$

To acquire images, stained cell samples (5 μL) were placed between glass slides and observed under transmitted light by using a confocal laser scanning microscope (Zeiss LSM 700).

2.11. Hemocompatibility tests

In order to evaluate samples hemocompatibility, blood clot formation assay, tromboelastogram, and scanning electron microscopy (SEM) analysis were performed. All the experiments were run using the blood from 4 human healthy donors, kindly provided by the transfusion center of Ospedale Maggiore della Carità, in Novara. The tests were run in triplicate for statistical significance.

For blood clot formation assay, samples were placed in 48-well plates and 50 μL of human blood were poured on them. After 1, 3, 5, 10 and 20 min 0.5 mL of ultrapure water were added, and 100 μL of the mix were used for spectrophotometric analysis at 450 nm. Absorbance values were inversely proportional to blood coagulation.

Tromboelastogram was obtained pouring on the air dried SPI/agarose/polyphenols hydrogels 1 mL of human whole blood for 30 min at 37 °C. The blood was then collected and added to Kaolin to increase coagulation speed. 0.34 mL of the mix were placed into cuvette with 20 μL of a 0.2 M $CaCl_2$ solution. The mix was analyzed with Tromboelastograph (TEG 5000, Haemonetics, USA), giving 4 parameters that is clot starting time, coagulation time, coagulation speed, and clot strength.

Samples used for tromboelastograph test were then treated for SEM analysis. Samples were washed two times with 0.2 M cacodylate buffer (pH 7.4), then fixed with Karnovsky buffer (8% formalin, 2.5% glutaraldehyde, in 0.2 M cacodylate buffer, pH 7.4) for 30 min. Subsequently, samples were rinsed with cacodylate buffer and dehydrated with increasing concentrations of ethanol (from 50% to 100%). Finally, samples were soaked in hexamethyildisilazane for 16 h. Samples were finally observed with JSM-IT500 InTouchScope™ Scanning Electron Microscope (JEOL, Tokyo, Japan).

2.12. Scratch test

Wound healing activity of SPI/polyphenols materials was evaluated in vitro as previously described [32]. Human HaCaT keratinocytes were seeded into 8-well chamber (Nunc™ Lab-Tek™ Chambered Coverglass) at a density of 300 000 cells/well in 0.3 mL medium per well. Following an incubation of 24 h at 37 °C, cells monolayers were wounded with a pipette tip to remove cells from a specific region of the monolayer. The culture medium was then removed, and the cells were washed twice with PBS. Cells were then incubated with fresh culture medium containing agarose (0.625 mg/mL) or agarose as above/0.875 mg/ml SPI or agarose/SPI as above/0.0875 mg/ml CGA/0.005 mg/ml CA or GA. Wound closure was evaluated using an inverted microscope (Zeiss LMS 700, Carl Zeiss, Germany) at t_0 and t_{24} h of incubation by measuring the areas at these times. Wound closure is expressed as the ratio of the areas at t_0 and t_{24} h for each sample. The values obtained from three independent experiments were averaged and the standard error of the mean was calculated to account for reproducibility.

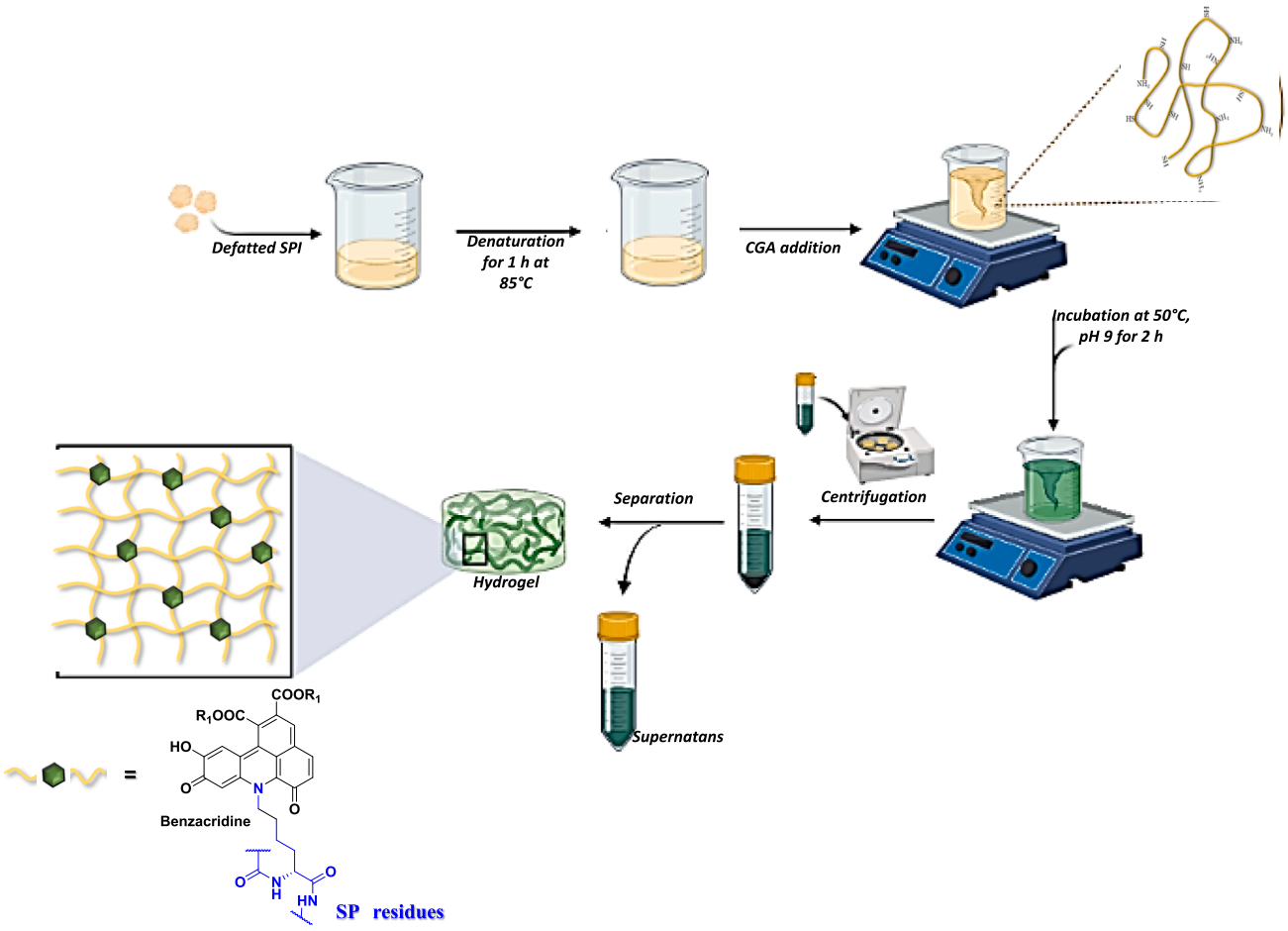

Fig. 1. Schematic outline of the procedure for the preparation of SPI/polyphenols glues exemplified for CGA; shown is also the supposed mechanism of interaction of CGA with the SPI residues.

2.13. Antibacterial activity

2.13.1. Bacterial strains and growth conditions

Bacterial strains *Staphylococcus aureus* ATCC 12600, Methicillin Resistant *Staphylococcus aureus* (MRSA) WKZ-2, *Staphylococcus epidermidis* ATCC 35984, *Acinetobacter baumannii* ATCC 9606 and *Pseudomonas aeruginosa* ATCC 27853 were grown in Muller Hinton Broth (MHB, Becton Dickinson Difco, Franklin Lakes, NJ, USA) and on LB Agar (Tryptone 10 g/L; yeast extract 10 g/L; sodium-chloride 5 g/L). In all experiments, to assess the antimicrobial activity of air-dried SPI/agarose/polyphenols hydrogels, bacterial cells were inoculated and grown overnight in MHB at 37 °C. The next day, bacteria were transferred to a fresh MHB tube and grown to mid- logarithmic phase.

2.13.2. Inhibition halo and percentage of bacterial growth

To evaluate the inhibition halo of air-dried SPI/agarose/polyphenols hydrogels, bacterial cells were diluted into 0.5x nutrient broth (NB) to approximately 2×10^8 CFU/mL and inoculated into LB plates. A square of 1 cm^2 of the hydrogels was then placed on the inoculated plate and pressed to ensure full contact with the agar surface. Plates were then incubated at 37 °C overnight and the bacterial growth around the hydrogels was evaluated. To assess the percentage of cell viability, bacterial cells were diluted into 0.5x NB to approximately 2×10^6 CFU/mL. 500 μL of the bacterial culture were placed on a 1 cm^2 square of each hydrogels tested and incubated 37 °C overnight. The next day, each culture sample was diluted in 0.5xNB medium and plated on LB agar to perform the colony counting.

2.14. Statistical analysis

Statistical analysis was performed by using a Student's *t*-Test. Significant differences were indicated as *($P < 0.05$), **($P < 0.01$) or ***($P < 0.001$).

3. Results and discussion

3.1. Design rationale

Initial experiments were devoted at development of the optimal conditions for glues preparation from SPI using the selected polyphenols of natural origin. Previous studies using SPI for preparation of adhesives adopted alkaline pH conditions as those obtained by addition of 1–8 M urea and guanidine to favour protein denaturation and improve mechanical properties [30]. Protein denaturation is essential to favour exposure of the aminoacidic residues, particularly lysine amino groups, to the medium, allowing interaction with additives or cross linkers. In the present study interaction of aminoacidic residues with polyphenols and their oxidation products was expected to modify the properties of SPI. Use of strong alkaline conditions was discarded to avoid oxidative degradation of the polyphenols and their oxidation products as well as to make the glue preparation conditions compatible with their use in tissue repair. Systematic investigation of thermal denaturation conditions allowed to select proper treatment of SPI and a protocol was eventually developed for preparation of glues from SPI incorporating the polyphenols. The choice of the polyphenols, i.e. caffeic acid (CA),

Table 1
List of the SPI based hydrogels and glues prepared in the present work and their chemical composition.

SPI/polyphenols ***glues***	
Chemical components	Acronym
Soy protein (CTRL)	**SPI**
Soy protein with chlorogenic acid	**SPI/CGA**
Soy protein with caffeic acid	**SPI/CA**
Soy protein with gallic acid	**SPI/GA**
SPI/Agarose/polyphenols ***hydrogels***	
Chemical components	Acronym
Soy protein and Agarose (CTRL)	**SPI/agarose**
Soy protein, Agarose with chlorogenic acid	**SPI/agarose/CGA**
Soy protein, Agarose with caffeic acid	**SPI/agarose/CA**
Soy protein, Agarose with gallic acid	**SPI/agarose/GA**

Table 2
Underwater resistance of wood specimens and chicken muscle slices glued with SPI or SPI/polyphenols. Shown are the mean of experiments in triplicate. SD ± 1.

Underwater resistance (days)				
Adherend	*SPI*	*SPI/CA*	*SPI/CGA*	*SPI/GA*
Wood specimens	1	9	22	5
Chicken muscle slices	1	5	7	15

Table 3
Lap shear strengths of single lap wood joints glued with SPI-based adhesive, and a reference vinyl adhesive.

Sample	**Lap shear strength (Mpa)**
SPI/urea	2.07 ± 0.70
SPI/CGA	2.16 ± 0.41
Vinyl adhesive	4.02 ± 0.83
SPI /CA	3.21 ± 0.19
SPI/ GA	2.40 ± 0.37

chlorogenic acid (CGA) and gallic acid (GA), was guided by consideration of their availability, the widespread occurrence in plant sources and sufficient knowledge of the oxidation chemistry.

In brief, SPI was dissolved in water (at 10% w/w) and taken for 1 h at 85 °C, a temperature at which protein denaturation occurs. The polyphenol component was then added, and the final solution brought to 50 °C and to pH 9 and taken in air for 2 h. Under these conditions a smooth oxidation of the polyphenol component is expected to take place. The final concentration of the polyphenol was selected based on experiments carried out over the range 10–30 mM aimed at optimizing polyphenol consumption. During this treatment a glue is formed that acquires a consistency higher than that of SPI subjected to the same conditions, but in the absence of the polyphenols.

Clear evidence of the interaction of SPI with the polyphenol was obtained in the case of CGA from the development of a bright green color in the glue that was formed. Generation of benzacridine pigments by oxidative coupling of caffeic acid esters including CGA in the presence of amines and amino groups of proteins has been described previously [33] (Fig. 1). On the other hand, aerial oxidation of CGA under the same conditions gave a brown solution indicating the involvement of the protein in the green pigment formation. (Figure S3).

The optimized protocol was extended to the other polyphenols selected. The glue obtained in the presence of caffeic acid and gallic acid were yellowish brown in color (Figure S4). In all cases the glue was recovered by centrifugation of the final mixture to remove the supernatants. These latter were subjected to spectrophotometric analysis to evaluate the consumption of the starting polyphenol that proved almost complete for all the polyphenols (data not shown).

All the materials prepared in this study are summarized in the following Table 1.

3.2. Mechanical properties

A preliminary evaluation of the properties of the materials prepared as glues and their underwater resistance was obtained by a simple test involving application of the adhesive on wood specimens that are then pressed together with a clamp for 24 h and soaked in water (Figure S5). They were periodically checked till detachment of the wood specimens.

The resistance of the glue obtained from SPI/CGA was 22 days, a value to be evaluated against that of SPI subjected to the same treatment, but in the absence of additives, that was only about 24 h. A lower resistance was exhibited by SPI/CA and SPI/GA glues with values of 9 and 5 days, respectively, as reported in Table 2.

The failure stress of the adhesive was determined by measuring the lap shear strength, which corresponds to the failing load divided by the bond area (in these experiments 4.0 cm^2) by use of an Instron testing machine. The failure modes for all test specimens showed a cohesive failure within the adhesive, as shown in Figure S6 for the SPI/CGA sample, which highlighted the good interaction between adhesive and wood substrate. The results of lap shear tests are reported in Table 3. SPI Urea glue described in previous reports for its good performance [30] was also tested for comparative purposes. The soy protein-based adhesive samples showed stress values ranging from 2.1 (SPI/urea) to 3.2 (SPI/CA) MPa. The remarkable performance of SPI/CA is likely related to the comparatively more compact morphology of this sample that showed a homogeneous and dense structure, as highlighted by SEM observations (see section 3.3). Under the same experimental conditions, a commercial vinyl acetate-based adhesive used as control yielded a value of 4.0 Mpa, while strengths of 2.0–2.5 MPa have been recently reported for polyamidoamine-epichlorohydrin and tannic acid -cross-linked soybean meal adhesive [34], confirming the good performance of the SPI samples reported herein.

In further experiments the underwater resistance of the SPI/polyphenols glues was tested using chicken skin that has been subjected to a defatting treatment and repeatedly washed as previously described (Figure S7) [31]. Yet, the underwater resistance proved in all cases quite poor with values not exceeding 30 min. On this basis other experimental conditions were explored that seemed also more relevant to the potential use as surgical glues. Slices of chicken breast muscle were glued by application of the SPI/polyphenols glues that have been subjected to curing by drying in air for 6 h, and then immersed in PBS. The results shown in Table 2 indicated adhesive/cohesive properties of SPI/polyphenols glues, the best results observed with GA, but also with CGA the resistance was satisfactory. The difference in the nature of the adherends clearly accounts for the responses observed in the wet resistance test and, more importantly, in all cases the performance of the SPI/polyphenols materials were superior with respect to SPI alone.

Furthermore, the viscoelastic properties of the SPI-based adhesive were assessed by oscillatory rheology. The interval of linear viscoelasticity of the gels was preliminary determined, and a value well above 10% strain was recorded (Figure S8). Frequency sweep tests were then performed at 2% strain to gather information on the dependence of storage (G′) and viscous (G″) moduli, and complex viscosity η* on the frequency (Fig. 2a, 2b).

For all samples, both G′ and G″ displayed a negligible change with increasing frequency over the explored frequency range, suggestive of the presence of a crosslinked structure. Additionally, G′ values were about 1 order of magnitude higher than those of G″, indicating a predominantly elastic, solid-like behavior of the glues. In particular, for all samples storage the modulus values were above 1000 Pa, while loss moduli were in the 200–500 Pa range, due to a moderate degree of physical or chemical cross-linking.

Such viscoelastic features are suitable for applications requiring stiffness and resilience [35], and the measured values were significantly higher than G' values found for SPI water dispersions [36] yet comparable to those measured for SPI hydrogel containing processed spirulina platensis as a mechanically structuring additive [37]. From a

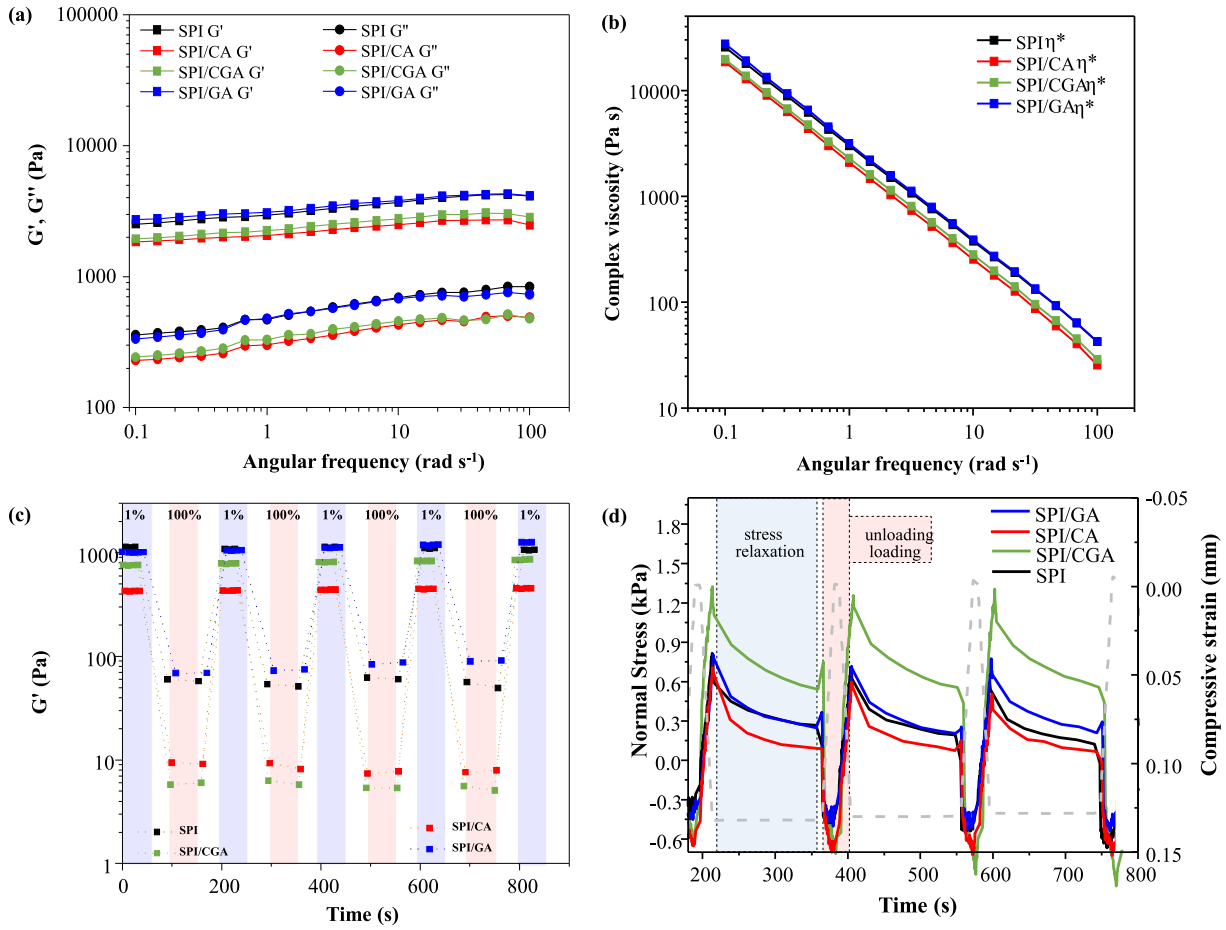

Fig. 2. Dependence of (a) viscoelastic moduli and (b) viscosity on the angular frequency; (c) G' values of the glues calculated from alternating 1% and 100% strain time sweep experiments; (d) cyclic uniaxial loading–unloading curves of the glues.

comparison of the equilibrium shear modulus of the hydrogels, measured at the low-frequency limit value of G′, it turned out that SPI/CGA and SPI/CA displayed lower viscoelastic properties (1950 and 1840 Pa, respectively) than SPI (2530 Pa), while SPI/GA was even stiffer than the latter (2730 Pa). This apparently odd behaviour suggests that the viscoelastic properties of the hydrogels depend on several factors, including the dilution effect of the polyphenol addition which causes the moduli values to decrease, and the crosslinking reaction between phenols and the SPI residues responsible for a tighter structure. In the case of CGA and CA, the former effect was prevailing, with a partial disentanglement of the SPI chains, which led to lower moduli values. On the other hand, GA reacted more efficiently with the amino groups of SPI (see Section 3.3 and Fig. 3a), resulting in a hydrogel with higher viscoelastic properties.

The complex viscosity values (η*) of the SPI-based glue decreased with increasing frequency (Fig. 2b), proving the shear thinning behavior of the samples, stemming from the weakening of the intermolecular forces within the gel which triggers molecular motion at higher shearing rates. The complex viscosity values also confirmed that SPI/GA and SPI glues were tighter compared to SPI/CGA and SPI/CA. As an example, at 10 rad s SPI/GA displayed a value of 388 Pa s, to be compared with 253 Pa s of SPI/CA. The slope of η* as a function of the angular frequency is a parameter which describes the resistance of the gel to flow and measures the deviation of the fluid from the Newtonian behavior [38]. Generally, polymer systems with low slope values have higher entanglement density and are more difficult to disentangle under shear [39]. The slope values of the SPI-based glues were in between 0.91 and 0.92, indicating that all samples are prone to flow when subject to a shearing force, thus confirming the feasibility of their use as tissue adhesives.

Furthermore, since the self-healing property is important for a glue to be used in wound healing, time sweep tests with alternating strain extents (1 and 100%) were performed to investigate the glue ability to reconstruct their structure after large deformations [40] As noticed from Fig. 2c, when the hydrogel were subjected to high strain values, G' abruptly dropped by about 1 order of magnitude, resulting even lower than G'', due to the network disruption. When the oscillation strain was reverted to 1%, the structure of the hydrogel was reconstructed, as demonstrated by the reversible increase of G', suggesting that the hydrogels were able to self-heal.

The adhesive properties of the glues were preliminary assessed by subjecting them to cyclic compression tests (Fig. 2d) using a rotational rheometer. All samples exhibited good mechanical stability, as they displayed constant stress values upon repeated compression. In order to gather some insight on the adhesive properties, the compression step was followed by a stress relaxation segment, which caused the compressive force to be partially released. During the subsequent unloading step, the normal force attained negative stress values (~0.6 kPa for SPI/CA and SPI/CGA), which demonstrate the good cohesive and adhesive properties of the glues [41].

3.3. Structural and morphological characterization

In order to get an insight into the mode of interaction of the polyphenols with the soy protein under the reaction conditions adopted, different characterization techniques were used. The amounts of SH and NH_2 groups in SPI further to the reaction with the polyphenols were determined by conventional chemical assays based on the Ellman's reagent and *o*-phthalaldehyde reaction, respectively, followed by

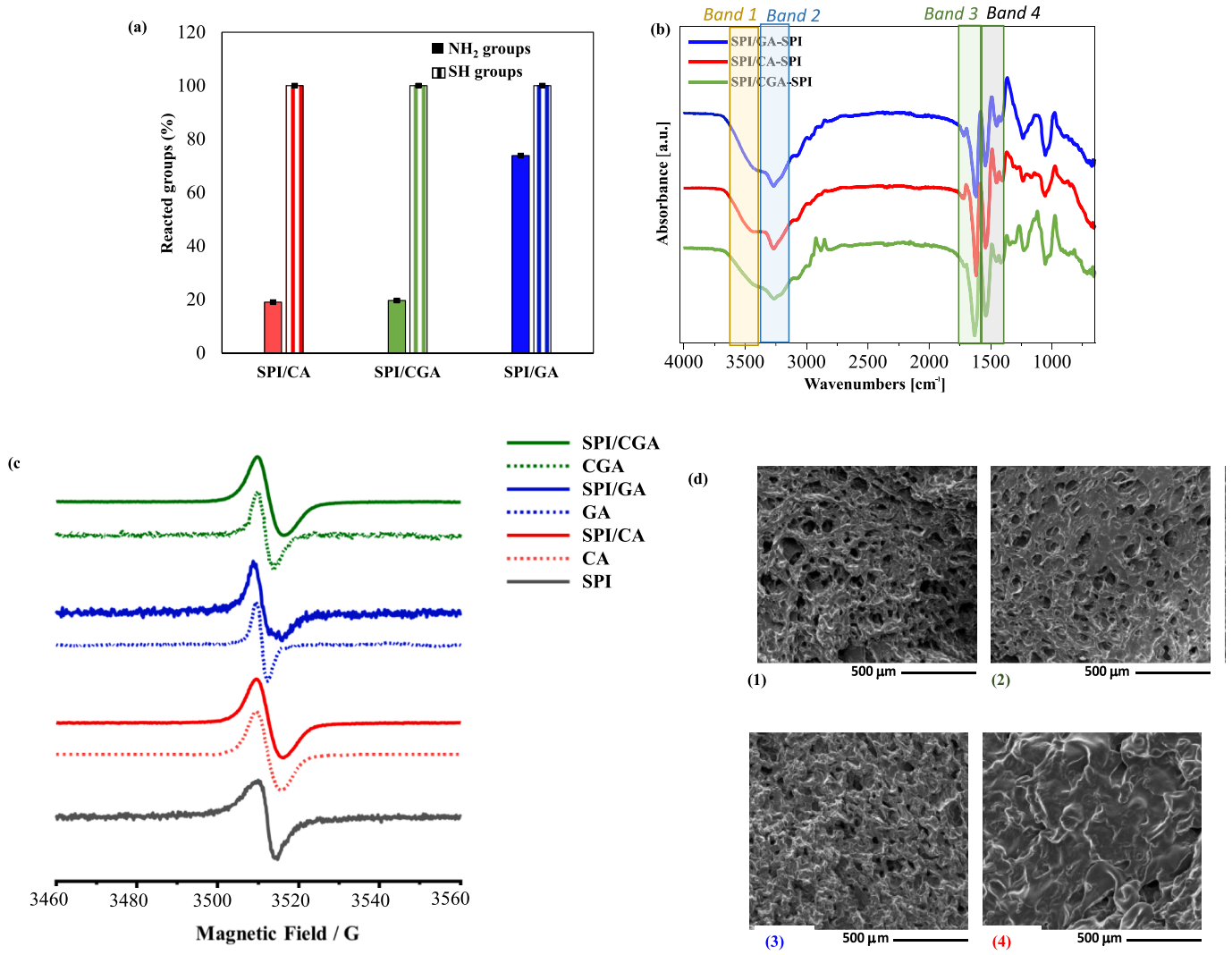

Fig. 3. **(a)** Percentage of reacted NH_2 and SH groups of SPI in SPI/polyphenols with respect to SPI. Shown are means of triplicates ± SD; **(b)** Differential spectra obtained by subtracting SPI spectrum from those of the SPI/polyphenols samples; **(c)** EPR spectra of SPI and SPI/polyphenols. Data for the materials obtained by oxidation of polyphenols at pH 9 in air in the absence of SPI (polyphenol polymers) are shown for comparison; **(d)** SEM images of SPI (panel 1), SPI/CGA (panel 2), SPI/GA (panel 3), SPI/CA (panel 4).

spectrophotometric determination. The plot in Fig. 3a shows a substantial involvement of SH groups in the SPI/polyphenols glues compared to SPI alone after denaturation. An SH content value of 1.8% w/w was evaluated for the denatured SPI based on a calibration curve using glutathione as reference thiol. As to the reacted amino groups, SPI/GA showed the highest involvement of these groups with respect to SPI followed by SPI/CA and its ester SPI/CGA. The content of NH_2 group of denatured SPI was 3% w/w as estimated based on a calibration curve built using alpha *N*–BOC lysine as a reference amino compound. For either assay the absorption contribution of the materials to the detection wavelength was duly considered. These results show an involvement of both the amino and sulfhydryl groups of SPI in the reaction with the species generated by oxidation of the polyphenols investigated to a variable extent. The covalent interaction of tannins featuring polyphenols moieties with amino groups of SPI residues have been previously documented by MALDI MS analysis [42]. Further insight into the mode of interaction of the polyphenols with SPI was provided by ATR FT-IR analyses that was carried out on the glues as lyophilized powders. Given the small amount of the polyphenol with respect to SPI in the final materials, differential ATR FT-IR spectra were considered as obtained by subtracting the SPI spectrum from those of the SPI/polyphenols (Fig. 3b). The spectra obtained for SPI and SPI/polyphenols are shown in Figure S9.

The main differences were noticed in the 3500–3000 cm^{-1} (*Band 2*) range and particularly in the region above 3300 cm^{-1} (*Band 1*), reflecting the involvement of the amino groups of SPI in the reaction with the polyphenols and their oxidation products [43]. The contribution of the OH groups of the polyphenol moieties to the complex broad band observed in this region should also be considered. Moreover, a change in the ratio of the bands at around 1625 cm^{-1} (*Band 3*), and 1545 cm^{-1} (*Band 4*), with respect to those observed for SPI alone, would indicate that bands due to C═O stretching of the carboxyl groups and the C═C stretching of the aromatic ring of the polyphenol components overlap and contribute to some extent to the dominating amide I and II band of the protein in the SPI/polyphenols materials. This observation is in line with previous reports indicating slight changes in the SPI main bands further to physical/chemical crosslinking with caffeic acid [44].

The SPI/ polyphenols glues were also subjected to EPR analysis. This represents the methodology of choice for detecting structural modifications in polymeric phenolic systems as reflected by the different type and amount of radicals arising from quinone/catechol disproportionation [45]. Preliminary analysis of denatured SPI showed an asymmetrical free-radical signal (Fig. 3c). Similar signals were reported in the literature and ascribed to carbon-centred radicals formed in the dry

Table 4
EPR spectral parameters of SPI and SPI/polyphenols glues as lyophilized powder. Data for the materials obtained by oxidation of polyphenols at pH 9 in air in the absence of SPI (polyphenol polymers) are shown for comparison.

Sample	Spin density/ g^{-1}	ΔB/G (±0.2)	Gaussian contribution	g-factor (±0.0003)
SPI/CGA	2.1×10^{17}	5.4	0.74	2.0040
CGA	2.7×10^{17}	3.9	0.72	2.0040
SPI/GA	9.8×10^{15}	6.7	0.35	2.0046
GA	1.9×10^{15}	3.0	0.49	2.0045
SPI/CA	3.1×10^{16}	6.2	0.72	2.0039
CA	1.0×10^{18}	6.1	0.64	2.0049
SPI	3.4×10^{15}	5.5	–	2.0027

protein during storage exposed to oxygen and trapped in the solid matrix [46,47].

In Fig. 3d spectra obtained from SPI/polyphenols (full lines) are shown in comparison with those of the polymers prepared from oxidative polymerization of the polyphenols alone under the same conditions used for SPI/polyphenols reactions (in air, pH 9, 50 °C, dotted lines). All spectra exhibit roughly a similar lineshape, i.e. a singlet at a g-factor value slightly higher than that observed for the denatured soy proteins (Table 4), suggesting the contribution of heteroatoms to the molecular orbitals in which the free-electrons are delocalized. The lineshapes are intermediate between the lorentzian and the Gaussian derivatives. A lorentzian lineshape is generated by the presence of a single population of equal radicals, while a Gaussian lineshape arises from the convolution of signal distribution; consequently, our results indicate that an ensemble of similar, but not completely equal, radical species contribute to the observed signal.

In the case of CA, an almost symmetric, broad signal is observed both in the presence and in the absence of soy proteins. The spin density is for both samples higher than that of the soy proteins. The decrease of spin density (2 order of magnitude) observed for the SPI/CA sample compared to CA polymer roughly reflects the amount of the CA-derived components present in the final material that is around 1%. The prevailing Gaussian line shape suggests a polydisperse nature of the radical centres, not altered by the presence of the protein.

The polymer from GA exhibits a narrow symmetric line, whose prevailing lorentzian lineshape reveals a relatively narrow dispersity of resonant radical nature. The GA polymer has a scarce attitude to stabilize radicals (note the low spin density). The asymmetric line registered in the SPI/GA clearly shows the superposition of the signals from the protein and the GA polymer, which also explains the seemingly increased signal broadness of the composite signal, quantified by the peak-to-peak distance in G. The spin density is for both samples of the same order of magnitude of that observed for the protein.

In the case of CGA, almost symmetric signals are observed for both the CGA polymer and the SPI/CGA. The spin density of the CGA polymer is in line with those reported for other polyphenol polymers [45] and notably remains unaffected in the SPI/CGA glue in spite of the approx 1% w/w content of the CGA derived species in the final material. In this case, the significant increase of broadness (ΔB from 3.9 to 5.4 G passing from the CGA polymer to the SPI/CGA) cannot be ascribed to the superposition of the weak protein signal. Consequently, our results indicate that the interaction of CGA oxidation products with the protein results in species featuring a marked radical character. For both samples the prevailing Gaussian line shape is suggestive of a polydispersity of the radical center nature.

Inspection of the normalized power saturation profiles (Figure S10) reveals a decrease at high microwave power for all samples, indicating that all the spins present in the samples have similar relaxation behavior. For CGA and GA, the materials obtained in the presence of the protein show shifts of the maximum to higher microwave power compared to those of the CGA or GA polymers, suggesting that the protein affects the relaxation behavior of the oxidation species thereof.

Overall, for all polyphenols, the presence of SPI affects the EPR spectroscopic parameters, indicating some interactions to occur between the proteins and the oxidative polymerization products. The different effects observed depending on the considered polyphenol suggest that different interactions can take place.

The microstructure of the SPI/polyphenols glues was investigated by SEM analysis (Figure S11). SEM images of samples are shown in Fig. 3d. The pristine SPI glue (Fig. 3d panel 1) shows a loose structure, with large and irregular macroporosity and pore size in the range 20–150 mm, indicating poor connection of protein molecules in the gel. The glues obtained from SPI with CGA or GA (Fig. 3d panel 2,3) still show the large presence of macropores, whose dimensions are comparable to those found for pristine SPI, but the formation of a more irregular and corrugated morphology, with several creases on the walls of the sample surface, is observed. A different microstructure was instead observed for the SPI/CA gel (Fig. 3d panel 4). In comparison to other samples, SPI/CA shows a more compact morphology, with only a few macropores on the sample surface, indicating that CA can promote the formation of a more homogeneous and dense protein gel structure. Such feature may well account for the good performance of the SPI/CA glue in the adhesive

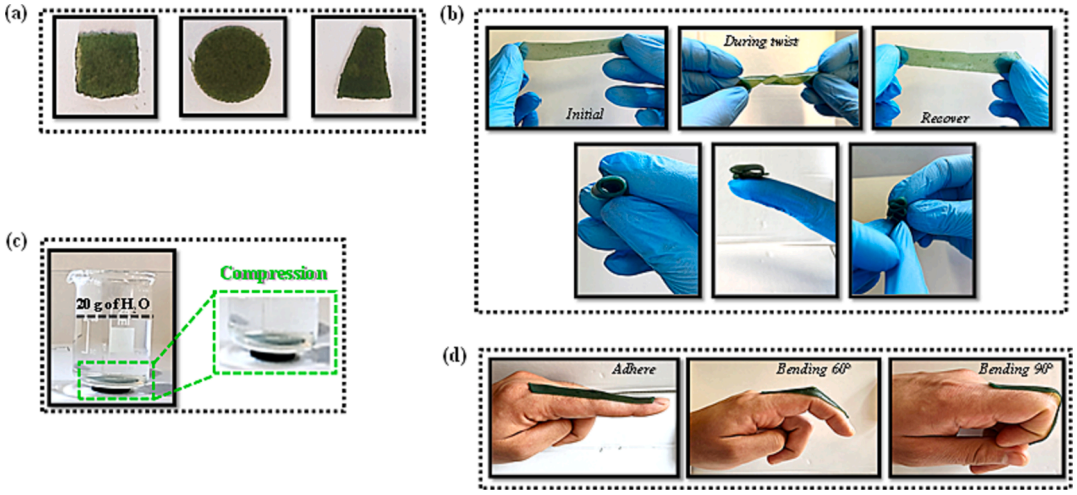

Fig. 4. Macroscopic demonstration of the physical properties of the SPI/agarose/CGA hydrogel: **(a)** Plasticity-shapeable properties of the hydrogel; **(b)** Mechanical performance of the hydrogel: bending and crossover stretching. The hydrogel quickly returned to its original shape after removing the twisting force; **(c)** Compressive strength with 20 g of H_2O; **(d)** The hydrogel tightly adhered to a human finger and accommodated its movements.

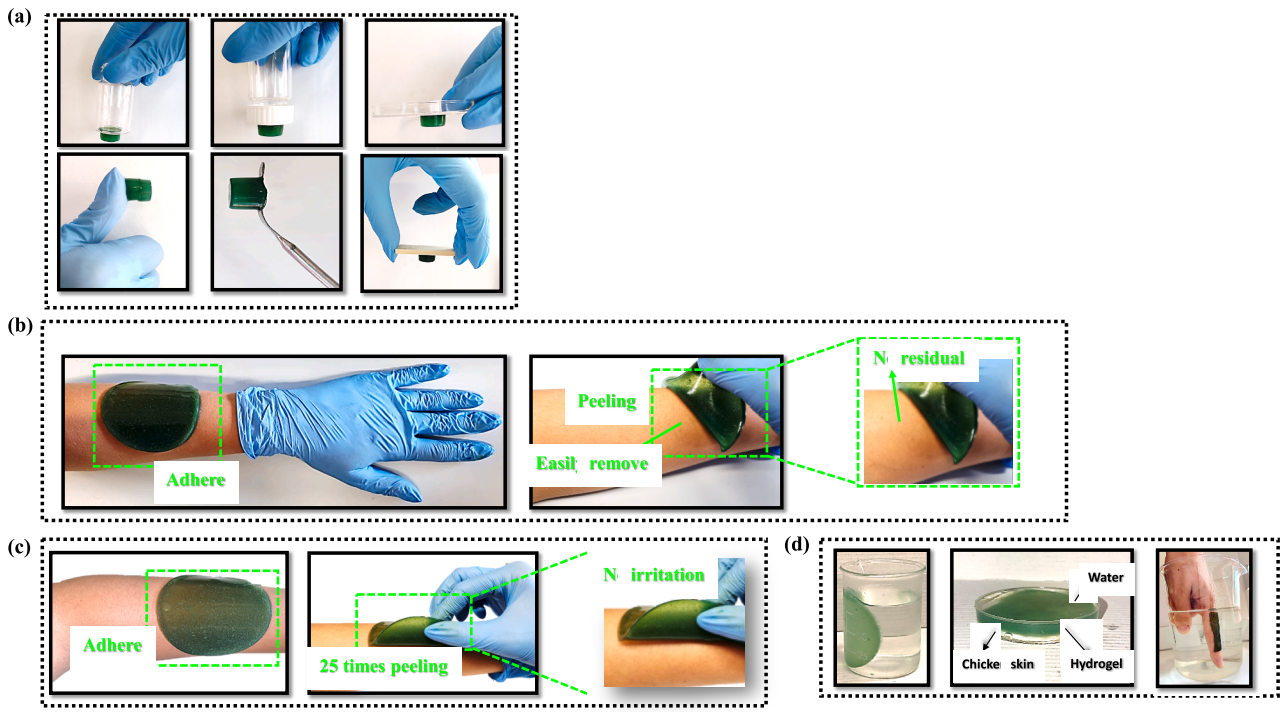

Fig. 5. Repeated adhesion properties of the SPI/agarose/CGA hydrogel: **(a)** Adhesion of the hydrogel to various materials; **(b)** The hydrogel exhibited no residue after being peeled from arm skin and **(c)** The hydrogel was repeatedly adhered to human skin showing no irritation; **(d)** Underwater resistance of SPI/agarose/CGA hydrogels on glass, chicken skin, human finger.

Table 5
WVP results of the hydrogels.

Sample	WVP (g/m Pa s)
SPI/agarose	$5.13 \pm 0.27 \times 10^{-12}$
SPI/agarose/CA	$4.64 \pm 0.22 \times 10^{-11}$
SPI/agarose/GA	$3.88 \pm 0.18 \times 10^{-11}$
SPI/agarose/CGA	$4.99 \pm 0.22 \times 10^{-11}$

tests described under Section 3.2.

3.4. SPI/agarose/polyphenols hydrogels

Encouraged by the interesting properties exhibited by the SPI/polyphenols glues we looked for expanding the potential application of these materials, e.g. for wound dressing use. To this aim different additives and reaction conditions for imparting resilience, stretchability and toughness to the materials were investigated. Finally, an optimized protocol was developed that used agarose as additional component.

An agarose/SPI hydrogel was prepared from an agarose solution in water and thermally denatured SPI at 70 °C. After cooling in a Petri dish, the resulting hydrogel was immersed in 10 mM water solution of the appropriate polyphenol at pH 9. In the case of CGA after 2 h the resulting gel develops a green color, due to the formation of the benzacridine species, indicating that CGA is able to permeate the hydrogel and to interact with SPI. The protocol developed was extended to the other polyphenols selected. All the hydrogels were dried in air, and then rehydrated before evaluation of their mechanical properties.

The hydrogels obtained under these conditions were translucent and smooth-faced, maintaining the exact shape of the mold. They exhibited good stretchability and excellent toughness. Subjected to compression force the hydrogel returned to its original cylindrical shape. Also, the mechanical properties of the hydrogel were very satisfactory. Owing to the excellent stretchability and compressive performance, the hydrogel could be applied on human joint with different bending without a feeling of any hindrance (one of the authors volunteered for these experiments). These properties are shown in Fig. 4 for the SPI/agarose/CGA hydrogel as representative example. Furthermore, the SPI/agarose/CGA hydrogel maintained these properties unaltered even after treatment for 1 h at different temperatures (-5°C, 25 °C, 37 °C, 50 °C) including those of relevance for its use for application on human body Figure S12.

The hydrogels showed a long term and repeatable adhesiveness to a variety of substrates both hydrophilic and hydrophobic in nature including glass, steel, polypropylene, polycarbonate (Fig. 5). Moreover, excellent adhesive performance was observed on the skin surface. Notably, the hydrogel sticking to the skin did not induce anaphylactic reactions. Moreover, the hydrogel could be peeled off without leaving any residue. The hydrogel maintained good adhesion even after 25 repeated peeling/adhering cycles. The adhesiveness to glass as well as to chicken and human skin was maintained also under water.

In view of the potential application of the air-dried SPI/agarose/polyphenol hydrogels as wound dressing devices the water vapor permeability (WVP) was measured.

Generally, the addition of an additive in a polymer hydrogel can modify its properties by reducing the intermolecular interactions between the polymer chains or by creating structural defects, which increase the WVP of the hydrogels.

Based on the data listed in Table 5, the addition of all the polyphenols in the hydrogel formulations led to an increase in water vapor permeability of about 1 order of magnitude with respect to SPI/agarose. This was likely due to the clustering of the polyphenol molecules in the polymer matrix, resulting in a discontinuous structure of the hydrogels. The obtained values of WVP were about two orders of magnitude greater than those reported for the films made from commodity polyolefins such as low- and high-density polyethylene.

3.4.1. Tensile properties

Tensile properties of SPI/agarose and SPI/agarose/polyphenol hydrogels were also investigated (Fig. 6). Representative stress–strain

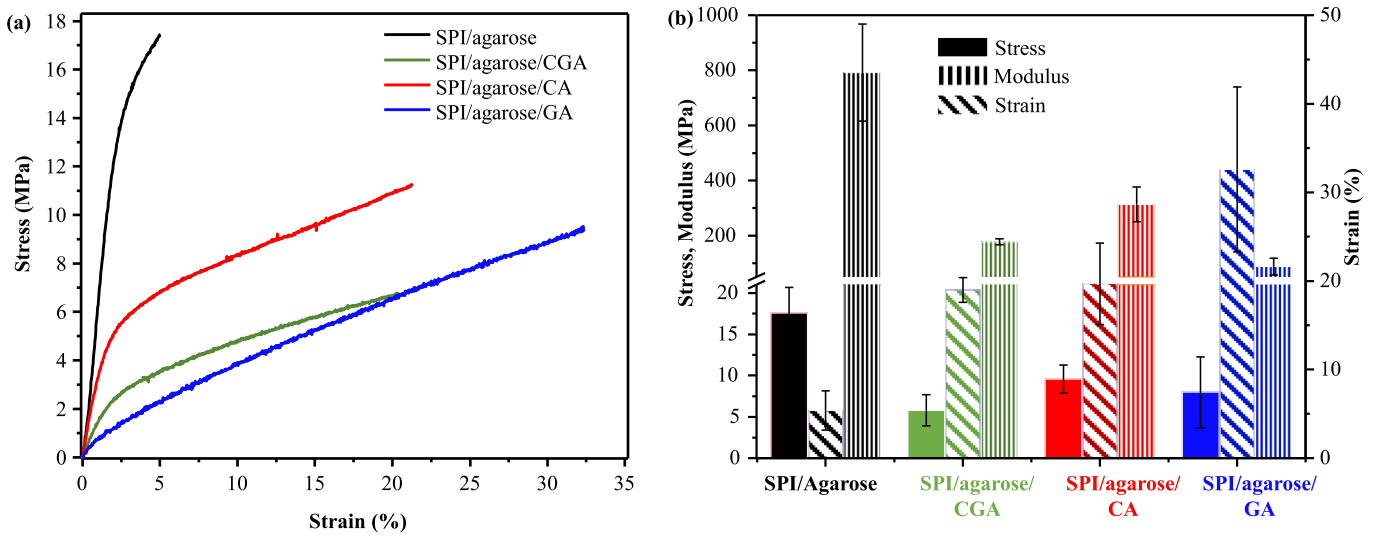

Fig. 6. Tensile properties of SPI/agarose of the SPI/agarose/polyphenols hydrogels. **(a)** Representative stress–strain curves; **(b)** Plot of the calculated tensile parameters.

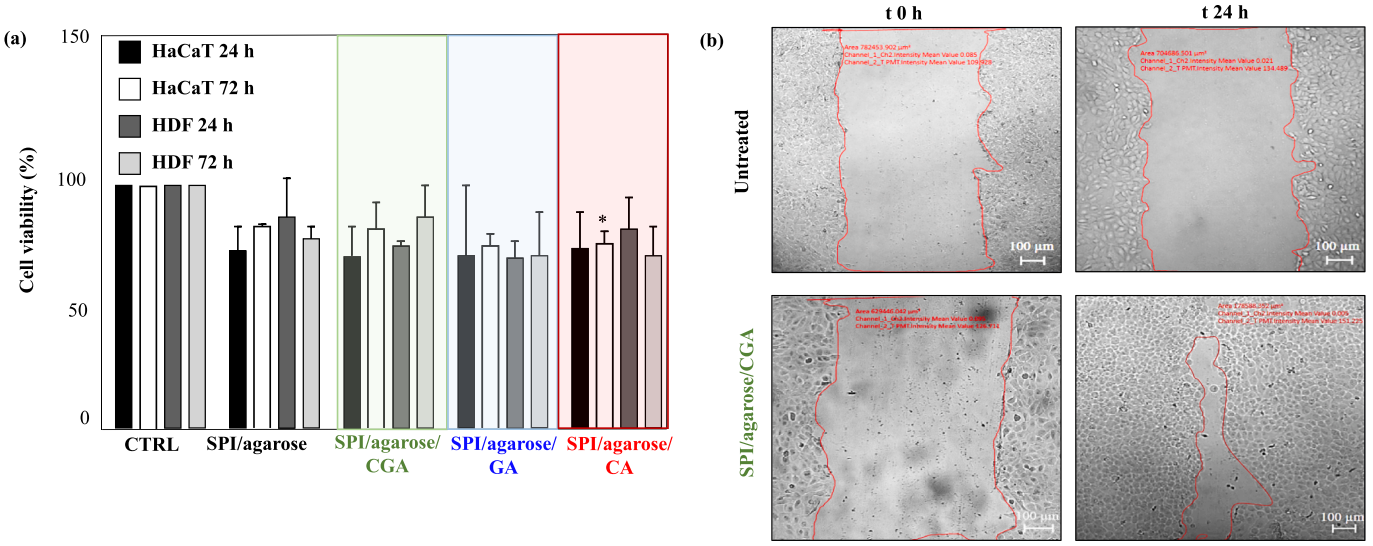

Fig. 7. **(a)** Biocompatibility of SPI based hydrogels on HaCaT and HDF cells after 24 and 72 h of incubation. Cell viability was assessed by MTT assay and expressed as the percentage of viable cells with respect to controls (untreated cells). Error bars indicate standard deviations obtained from at least three independent experiments, each one carried out with triplicate determinations. **(b)** Wound healing activity of SPI-hydrogels on HaCaT cells monolayer. Cells were wounded prior to treatment with each compound for 24 h. Images were acquired at t_0 and t_{24} h of incubations.

Table 6
Percentage of closure expressed as the ratio of the areas at t_0 and t_{24} h evaluated using Zen Lite 2.3 software. *P < 0.05 was obtained for control versus treated samples.

Sample	Reduction of Area (fold)
CTRL	0.97 ± 0.03
SPI/agarose/CGA	1.35 ± 0.01*
SPI/agarose/CA	1.01 ± 0.03
SPI/agarose/GA	0.96 ± 0.04
SPI/agarose	0.77 ± 0.49

curves of the films are shown in Fig. 6a, while the calculated tensile properties are summarized in Fig. 6b. Due to remarkable influence of the humidity relative content to the mechanical properties of the hydrogels, the tensile tests were performed at 50% RH. SPI/agarose exhibited tensile modulus and stress at break values of about 800 and 18 MPa, respectively, which are comparable to those reported for glycerol-modified soy protein isolate films [48]. The low strain at break value (about 5%) highlighted the brittle nature of SPI, due to the absence of plasticizers. Incorporation of phenol crosslinkers significantly impacted the mechanical behavior of the SPI hydrogels. In particular, a decrease in tensile modulus and stress was noticed for all SPI/agarose/polyphenols hydrogels, alongside an increase in their deformability. As an example, in the case of SPI/GA modulus dropped to<100 MPa, while elongation at break increased to about 33%. Therefore, the polyphenols acted as plasticizers for SPI, as they might hinder the intermolecular interactions between SPI chains, and the occurrence of chain cross-linking also favored their unfolding under uniaxial stress, resulting in reduced tensile strength and increased ductility [49].

3.4.2. *Cytocompatibility and wound healing properties*

To assess the therapeutic potential of SPI/agarose/polyphenols hydrogels, we analyzed their cytotoxic effects towards human

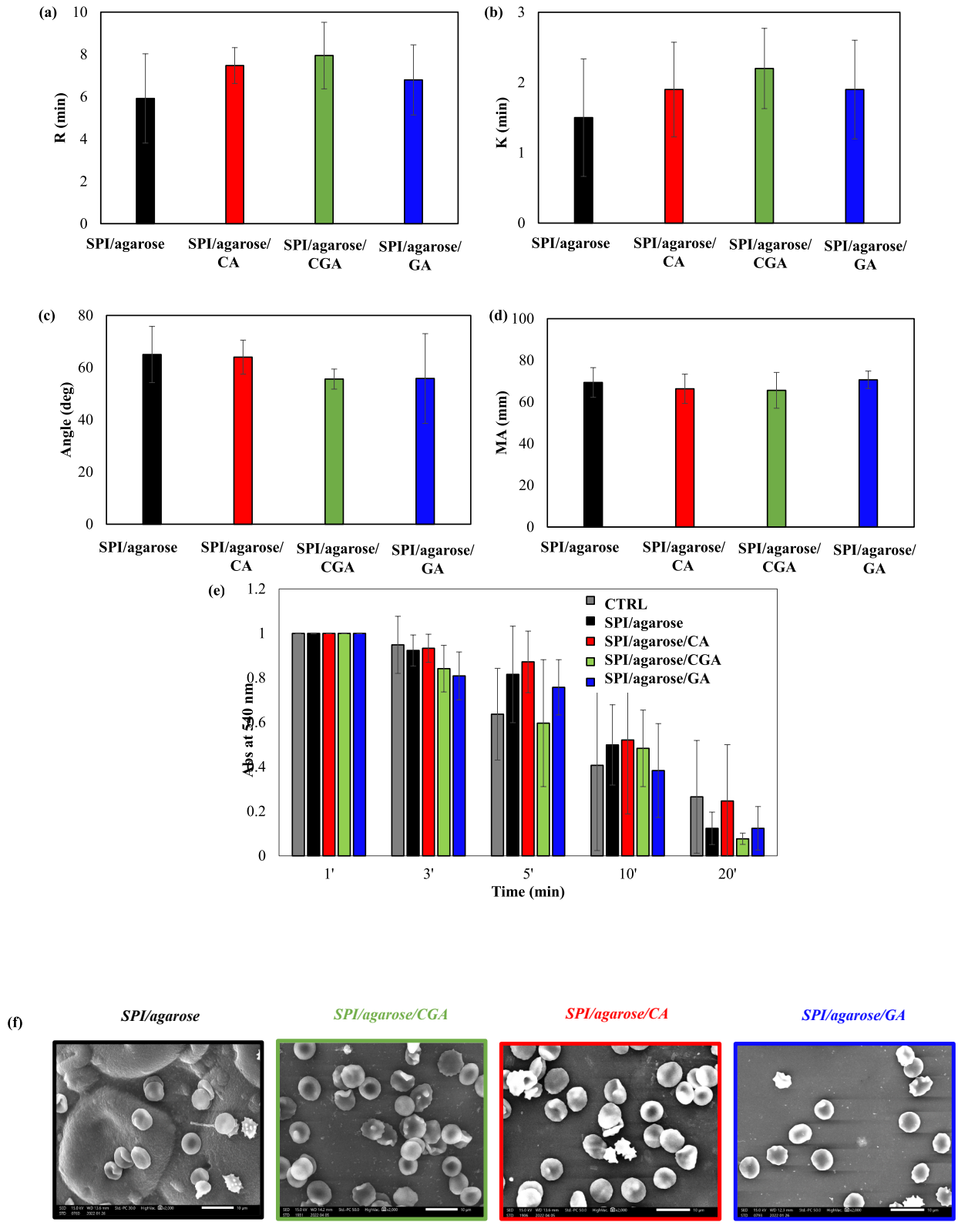

Fig. 8. Coagulation Parameters: **(a)** Reaction time (R)**; (b)** Coagulation time (K); **(c)** Coagulation velocity (alpha angle); **(d)** Clot strength (MA) **(e)** Clotting time of SPI/agarose hydrogels with and without polyphenols. **(f)** SEM images of SPI/agarose with and without polyphenols in the hemocompatibility test.

keratinocytes (HaCaT cells) and Human Dermal Fibroblasts (HDF cells) (Fig. 7a). A slight toxicity was detected at the concentrations of the SPI/agarose/polyphenols tested, even if it appeared not statistically significant. To confirm this, we also performed Trypan blue exclusion test experiments to discriminate between live and dead cells upon treatment with SPI/agarose/polyphenols hydrogels. No significant alteration of the cell viability was observed in all the conditions tested and the portion of dead blue cells appeared similar in all the samples and comparable to that observed for control HaCaT and HDF cells (Figure S13).

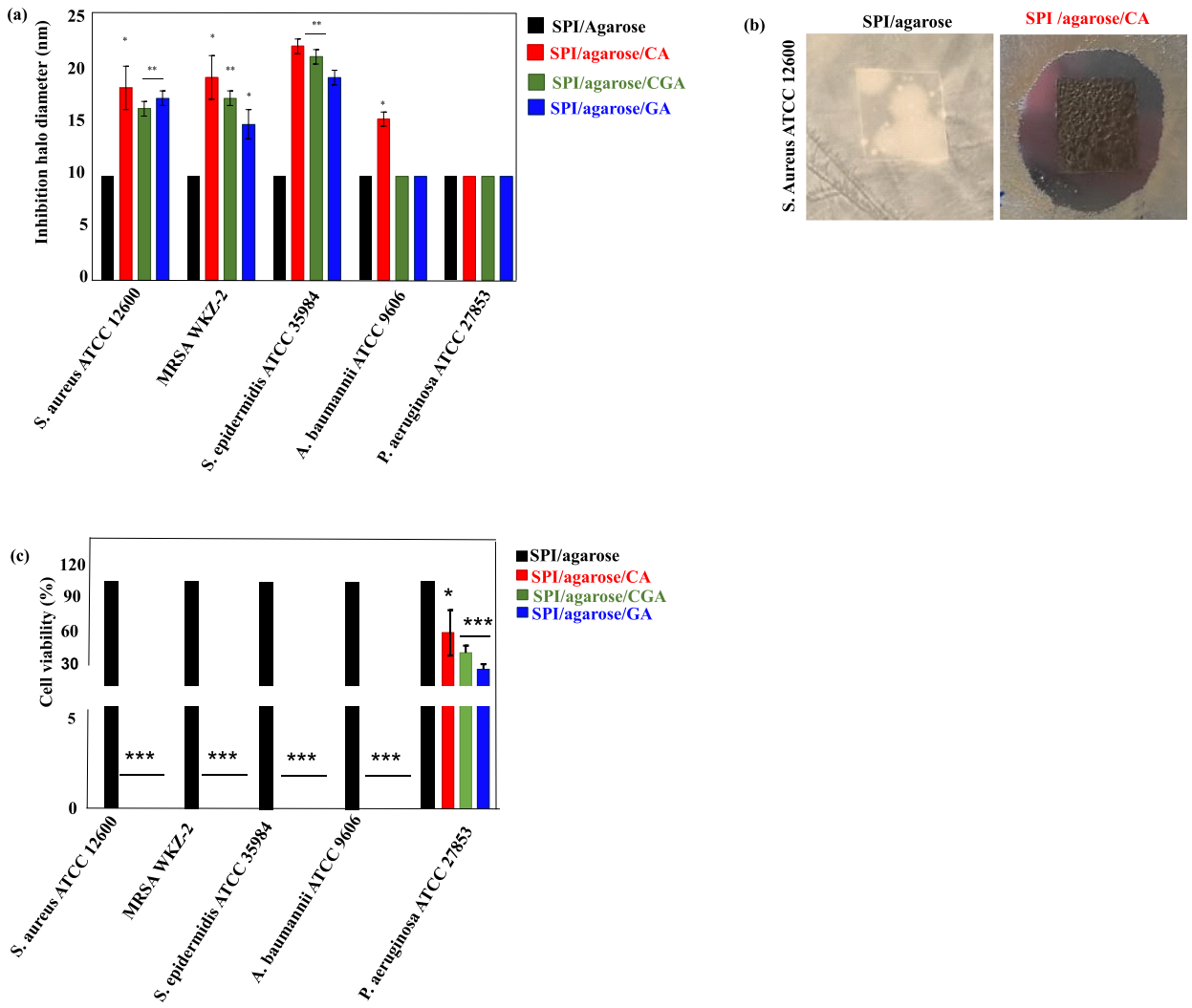

Fig. 9. (a, b) Antimicrobial activity of SPI/agarose-based hydrogels. Agar diffusion assays were performed and the diameter of zones of inhibition were calculated and reported for each sample. (c) Experiments were also performed by determining the ability of samples to inhibit bacterial growth in liquid medium used. Each graph refers to at least a biological duplicate and statistical analyses were performed by using Student's *t*-test. Significant differences were indicated as *P < 0.05, **P < 0.01 or ***P < 0.001.

We also performed experiments to test whether the hydrogels were able to stimulate wound re-epithelialization by human keratinocytes (HaCaT cell line). To this purpose, we performed an in vitro wound healing assay to evaluate hydrogel effects on cell migration. HaCaT cell monolayers were wounded with a pipette tip to remove cells from a specific region of the monolayers. Cells were then washed with PBS and incubated with different mixtures of the SPI/polyphenol hydrogel components. Fig. 7b shows the images of wound healing experiment on control cells, and on cells treated with SPI/polyphenols, CGA chosen as a most representative example, acquired at t_0 and t_{24} h of incubations. The percentage of closure was calculated as the ratio of the defect area at the final time with respect to the starting time as determined by using Zen Lite 2.3 software for the cells treated with each SPI/polyphenol system. Values in Table 6 are the mean of triplicates. As shown in Fig. 7b and reported in Table 6, SPI/CGA hydrogels were capable of significantly reducing the closing rate of the scratched area in human keratinocytes with respect to the untreated cells. On the other hand, no significant changes of wound healing rate were observed for the SPI/ hydrogels with the other polyphenols. This behaviour is apparently in contrast with the good wound healing ability of hydrogels loaded with GA or CA reported in literature [50–52], but the discrepancy may reasonably be accounted for considering the different chemistry of the interaction of these polyphenols with SPI under the conditions explored in this study compared with the other kind of polymers in which CA and GA were incorporated.

3.4.3. *Hemocompatibility*

To evaluate blood behaviour in contact with the hydrogels, hemocompatibility assays were performed (Fig. 8). TEG analysis considered four parameters: the reaction time namely the time between the start of the test and the beginning of coagulation process, physiologically comprised between 3.8 and 9.8 min; the coagulation time (K), that measures the length of the coagulation process, usually it is completed between 0.7 and 3.4 min; alpha angle, which represents the coagulation velocity and the physiological values are comprised between 47.8 and 77.7°, Maximum Amplitude (MA), which describes the clot strength and usually is between 49.7 and 72.7 mm. The results obtained from TEG analysis showed that all the hydrogels tested did not alter the physiological behaviour of the blood, because all the considered parameters were found inside the range of healthy blood. Moreover, there is no significant differences between the different hydrogels, which indicates that the polyphenols addition did not alter the hemocompatibility of SPI.

To further confirm the results obtained through TEG analysis, blood clot formation assay was performed. The results support the previous

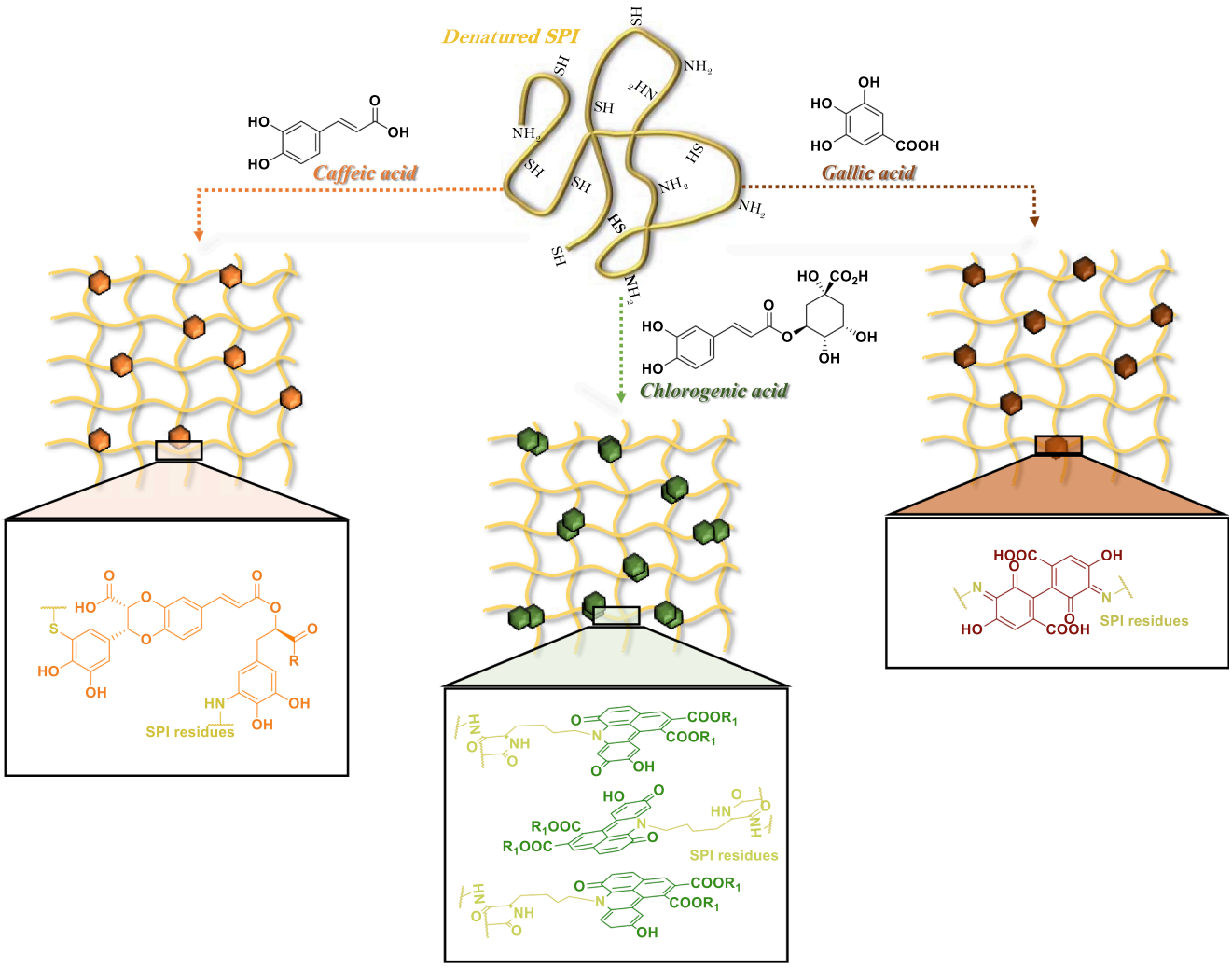

Fig. 10. Proposed mode of interaction of the polyphenols investigated with denatured SPI.

findings, because no significant differences were observed between controls and hydrogels, which means that also in this case blood natural behaviour was not altered by contact with SPI and polyphenols. The lack of differences between the polyphenols was also confirmed because no significant difference was shown by blood coagulation on the different hydrogels.

For all the samples SEM analysis displayed inactive platelets, alongside white and red blood cells. These results indicated that none of the hydrogels activated blood coagulation and further confirmed the previous results about the influence of the hydrogels on blood behavior. Overall, the results seem to indicate that the hydrogels, with or without polyphenols, did not affect blood coagulation.

3.4.4. Antibacterial activity

Air-dried SPI/agarose/polyphenols hydrogels were tested for their antimicrobial activity against a panel of ubiquitous pathogenic bacteria, such as *Staphylococcus*, *Acinetobacter* and *Pseudomonas* species. The ability of the SPI/Agarose-based hydrogels to inhibit bacterial growth was assessed by evaluating the appearance of the inhibition halo on inoculated plates (Figure S14). As reported in Fig. 9, all the hydrogels were able to induce the death of Gram-positive *Staphylococcus* species, either on *S. aureus* ATCC 12600, *S. epidermidis* ATCC 35984 or clinically isolated *MRSA* WKZ-2 strain. On the other hand, only the SPI/agarose/CA proved active against the Gram-negative *A. baumannii* ATCC 9606 strain.

To further investigate the antimicrobial activity, the percentage of bacterial growth in liquid medium was evaluated in the presence or in the absence of the hydrogels. An almost complete suppression of bacterial growth in the case of *Staphylococcus* and *Acinetobacter baumannii* strains (max. value 0.002048), and a complete death of *S. epidermidis* cells in the presence of SPI/agarose/CA and SPI/agarose/GA hydrogels were observed. Interestingly, all the hydrogels were able to significantly reduce the survival also of *Pseudomonas aeruginosa* cells, and more than 50% reduction was observed in the presence of the SPI/agarose/GA and SPI/agarose/CGA hydrogels.

Altogether, these findings suggest the possibility to employ the SPI-based hydrogels here described to counteract the growth of common pathogens, opening interesting perspectives to their applicability for topical treatment of bacterial infections.

3.5. Proposed model of the interaction of SPI with polyphenols

An insight into the nature of the interaction of the polyphenols with the protein under the aerobic oxidizing conditions developed was gained by a combined chemical, spectroscopic and microscopic approach. Based on all the evidence gathered it appears that a different chemistry can be envisaged for the three polyphenols investigated as summarized in Fig. 10. While in all cases the SH groups of denatured SPI are fully engaged in covalent interaction with the electrophilic units generated by polyphenol oxidation ensuring a tight cross linking of the protein with these components, the protein amino groups are involved to a different extent with the highest interaction being observed for gallic acid. The

oxidized quinonoid form of gallic acid is known to give rise to condensation with amino compounds rather than Michael type addition [53] as is shown in the Fig. 10 for oligomeric gallic acid derived species. The good performance of SPI/CA glues and the compact morphology of the hydrogel evidenced by SEM analysis may be accounted for by addition of the amino group to the *o*-quinone units of CA oxidation products as reported in the literature under comparable oxidation conditions [54].

Finally, the remarkable underwater resistance exhibited by the SPI/CGA hydrogels in wood specimen and animal tissues may be interpreted as the result of the hydrophobic character of the benzacridine units generated by interaction of oxidized dimeric CGA with amino groups. Such units may ensure a tight structure of the gel through dynamic pi-stacking interaction, but possibly also redox interaction as suggested by EPR analysis indicating the presence of a variety of species at different redox states capable of giving rise to stable carbon centred radicals.

4. Conclusions

In the present work we developed hydrogels from all natural accessible ingredients that is a protein fraction, the main industrial waste of soybean processing, and plant derived polyphenols, through an easy-to-do reaction requiring aqueous slightly alkaline medium under aerobic conditions. The hydrogels showed remarkable adhesive/cohesive properties, and an excellent underwater resistance under conditions of relevance for their use as surgical glues. Hydrogels endowed with good mechanical properties with a potential as wound dressing devices were obtained by inclusion of agarose in the formulation. These latter proved biocompatible, hemocompatible, not harmful to skin, and displayed durable adhesiveness. Additionally, they demonstrated excellent contact-active antibacterial properties and in some cases a favourable wound healing activity. The hydrogels described in the present work further expand the use of soy protein as the main component or additive for fabrication of devices intended for wound dressing as reported in recent research works [55,56] as they combine the advantages of the interaction of polyphenol derived products with SPI for ameliorating its mechanical properties, particularly underwater resistance with the biocompatibility and hemocompatibility of SPI [57].

Moreover, while confirming the favourable properties of polyphenols, particularly caffeic acid and gallic acid, in combination with biopolymers for wound dressing applications as reported in the recent literature [58–60], the results of the present study provide additional clues based on the different chemistry of interaction of the polyphenols with the SPI active residues for the interpretation of the observed effects and design of better performing materials. In this frame of particular interest is the SPI/CGA system that, based on the results of the wound healing experiments, the good antibacterial activity, and the satisfactory performance as tissue glue and bioadhesive, appears as a good candidate for further investigation in *in vivo* models.

Associated content.

CRediT authorship contribution statement

Rita Argenziano: Investigation, Data curation. **Sara Viggiano:** Investigation. **Rodolfo Esposito:** Investigation. **Martina Schibeci:** Investigation. **Rosa Gaglione:** Conceptualization. **Rachele Castaldo:** Investigation. **Luca Fusaro:** Investigation. **Francesca Boccafoschi:** Conceptualization. **Angela Arciello:** Methodology. **Marina Della Greca:** Conceptualization. **Gennaro Gentile:** Methodology. **Pierfrancesco Cerruti:** Methodology. **Gerardino D'Errico:** Methodology, Conceptualization. **Lucia Panzella:** . **Alessandra Napolitano:** Writing – review & editing.

Declaration of Competing Interest

The authors declare that they have no known competing financial interests or personal relationships that could have appeared to influence the work reported in this paper.

Data availability

Data will be made available on request.

Acknowledgments

This study was carried out within the Agritech National Research Center and received funding from the European Union Next-GenerationEU (PIANO NAZIONALE DI RIPRESA E RESILIENZA (PNRR) MISSIONE 4 COMPONENTE 2, INVESTIMENTO 1.4 D.D. 1032 17/06/2022, CN00000022). This manuscript reflects only the authors' views and opinions, neither the European Union nor the European Commission can be considered responsible for them.

Appendix A. Supplementary material

Calibration curve of Ellman's reagent and *o*-phthalaldehyde assay; SEM, EPR and ATR FT-IR analysis of SPI/agarose/ polyphenols hydrogels; the wood glued with SPI/CGA or SPI and the underwater resistance of the SPI/agarose/CGA hydrogel and SPI; pictures of SPI/CGA and SPI hydrogels after lyophilization; dry cup devices for water permeability test and picture of SPI/agarose/polyphenols hydrogels; Picture of SPI/Agarose/CGA hydrogels at different temperature; the inhibition halo images for each SPI/Agarose/polyphenol hydrogels. Supplementary data to this article can be found online at https://doi.org/10.1016/j.jcis.2023.08.170.

References

[1] Q. Guo, J. Chen, J. Wang, H. Zeng, J. Yu, Recent progress in synthesis and application of mussel-inspired adhesives, Nanoscale 12 (2020) 1307–1324, https://doi.org/10.1039/c9nr09780e.
[2] S. Suárez-García, J. Sedó, J. Saiz-Poseu, D. Ruiz-Molina, Copolymerization of a catechol and a diamine as a versatile polydopamine-like platform for surface functionalization: the case of a hydrophobic coating, Biomimetics 2 (2017), 22.
[3] J. Saiz-Poseu, J. Mancebo-Aracil, F. Nador, F. Busquè, D. Ruiz-Molina, The chemistry behind catechol-based adhesion, Angew. Chemie - Int. Ed. 58 (2019) 696–714, https://doi.org/10.1002/anie.201801063.
[4] M. Shin, J.Y. Shin, K. Kim, B. Yang, J.W. Han, N.K. Kim, H.J. Cha, The position of lysine controls the catechol-mediated surface adhesion and cohesion in underwater mussel adhesion, J. Colloid Interface Sci. 563 (2020) 168–176, https://doi.org/10.1016/j.jcis.2019.12.082.
[5] J. Chen, H. Zeng, Designing bio-inspired wet adhesives through tunable molecular interactions, J. Colloid Interface Sci. 645 (2023) 591–606, https://doi.org/10.1016/j.jcis.2023.04.150.
[6] X. Zhang, J. Chen, J. He, Y. Bai, H. Zeng, Mussel-inspired adhesive and conductive hydrogel with tunable mechanical properties for wearable strain sensors, J. Colloid Interface Sci. 585 (2021) 420–432, https://doi.org/10.1016/j.jcis.2020.10.023.
[7] X. Deng, B. Huang, Q. Wang, W. Wu, P. Coates, F. Sefat, C. Lu, W. Zhang, X. Zhang, A Mussel-Inspired Antibacterial Hydrogel with High Cell Affinity, Toughness, Self-Healing, and Recycling Properties for Wound Healing, ACS Sustain. Chem. Eng. 9 (2021) 3070–3082, https://doi.org/10.1021/acssuschemeng.0c06672.
[8] M.H. Kim, J. Lee, J.N. Lee, H. Lee, W.H. Park, Mussel-inspired poly(γ-gl utamic acid)/nanosilicate composite hydrogels with enhanced mechanical properties, tissue adhesive properties, and skin tissue regeneration, Acta Biomater. 123 (2021) 254–262, https://doi.org/10.1016/j.actbio.2021.01.014.
[9] H. Ruprai, A. Shanu, D. Mawad, J.M. Hook, K. Kilian, L. George, R. Wuhrer, J. Houang, S. Myers, A. Lauto, Porous chitosan adhesives with L-DOPA for enhanced photochemical tissue bonding, Acta Biomater. 101 (2020) 314–326, https://doi.org/10.1016/j.actbio.2019.10.046.
[10] J. Guo, W. Sun, J.P. Kim, X. Lu, Q. Li, M. Lin, O. Mrowczynski, E.B. Rizk, J. Cheng, G. Qian, J. Yang, Development of tannin-inspired antimicrobial bioadhesives, Acta Biomater. 72 (2018) 35–44, https://doi.org/10.1016/j.actbio.2018.03.008.
[11] D. Gan, W. Xing, L. Jiang, J. Fang, C. Zhao, F. Ren, L. Fang, K. Wang, X. Lu, Plant-inspired adhesive and tough hydrogel based on Ag-Lignin nanoparticles-triggered dynamic redox catechol chemistry, Nat. Commun. 10 (2019), https://doi.org/10.1038/s41467-019-09351-2.
[12] A. Cholewinski, F. Yang, B. Zhao, Algae-mussel-inspired hydrogel composite glue for underwater bonding, Mater. Horizons. 6 (2019) 285–293, https://doi.org/10.1039/c8mh01421c.
[13] C. Mortier, D.C.S. Costa, M.B. Oliveira, H.J. Haugen, S.P. Lyngstadaas, J.J. Blaker, J.F. Mano, Advanced hydrogels based on natural macromolecules: chemical routes

to achieve mechanical versatility, Mater. Today Chem. 26 (2022), 101222, https://doi.org/10.1016/j.mtchem.2022.101222.
[14] M. Friedman, D.L. Brandon, Nutritional and health benefits of soy proteins, J. Agric. Food Chem. 49 (2001) 1069–1086, https://doi.org/10.1021/jf0009246.
[15] S.Z. Lamaming, J. Lamaming, N.F.M. Rawi, R. Hashim, M.H.M. Kassim, M. H. Hussin, Y. Bustami, O. Sulaiman, M.H.M. Amini, S. Hiziroglu, Improvements and limitation of soy protein-based adhesive: a review, Polym. Eng. Sci. 61 (2021) 2393–2405, https://doi.org/10.1002/pen.25782.
[16] Y. Li, X. Huang, Y. Xu, C. Ma, L. Cai, J. Zhang, J. Luo, J. Li, J. Li, S.Q. Shi, Q. Gao, A bio-inspired multifunctional soy protein-based material: From strong underwater adhesion to 3D printing, Chem. Eng. J. 430 (2022), 133017, https://doi.org/10.1016/j.cej.2021.133017.
[17] G. Yildiz, J. Andrade, N.E. Engeseth, H. Feng, Functionalizing soy protein nano-aggregates with pH-shifting and mano-thermo-sonication, J. Colloid Interface Sci. 505 (2017) 836–846, https://doi.org/10.1016/j.jcis.2017.06.088.
[18] Y. Luo, Y. Wang, C. Xia, A. Ahmad, R. Yang, X. Li, S.Q. Shi, J. Li, M. Guo, A. K. Nadda, T. Ahamad, Q. Van Le, Eco-friendly soy protein isolate-based films strengthened by water-soluble glycerin epoxy resin, Prog. Org. Coatings. 162 (2022), https://doi.org/10.1016/j.porgcoat.2021.106566.
[19] Y. Zhao, L. Jin, X. Liu, X. Liu, S. Dong, Y. Chen, X. Li, X. Lv, M. He, Novel high strength PVA/soy protein isolate composite hydrogels and their properties, Front. Chem. 10 (2022) 1–10, https://doi.org/10.3389/fchem.2022.984652.
[20] Y. Yang, C. Zhang, X. Bian, L. Ren, C. Ma, Y. Xu, D. Su, L. Ai, M. Song, N. Zhang, Characterization of structural and functional properties of soy protein isolate and sodium alginate interpenetrating polymer network hydrogels, J. Sci. Food Agric. (2023), https://doi.org/10.1002/jsfa.12736.
[21] P. Dorishetty, R. Balu, A. Gelmi, J.P. Mata, N.K. Dutta, N.R. Choudhury, 3D printable soy/silk hybrid hydrogels for tissue engineering applications, Biomacromolecules 22 (2021) 3668–3678, https://doi.org/10.1021/acs.biomac.1c00250.
[22] B. Song, X. Fan, H. Gu, Chestnut-Tannin-Crosslinked, antibacterial, antifreezing, conductive organohydrogel as a strain sensor for motion monitoring, flexible keyboards, and velocity monitoring, ACS Appl. Mater. Interfaces. 15 (2023) 2147–2162, https://doi.org/10.1021/acsami.2c18441.
[23] W.X. Waresindo, H.R. Luthfianti, D. Edikresnha, T. Suciati, F.A. Noor, K. Khairurrijal, A freeze-thaw PVA hydrogel loaded with guava leaf extract: physical and antibacterial properties, RSC Adv. 11 (2021) 30156–30171, https://doi.org/10.1039/d1ra04092h.
[24] U.N. Tak, S. Rashid, P. Kour, N. Nazir, M.I. Zargar, A.A. Dar, Bergenia stracheyi extract-based hybrid hydrogels of biocompatible polymers with good adhesive, stretching, swelling, self-healing, antibacterial, and antioxidant properties, Int. J. Biol. Macromol. 234 (2023), 123718, https://doi.org/10.1016/j.ijbiomac.2023.123718.
[25] E. Kim, J.S. Jung, S.G. Yoon, W.H. Park, Eco-friendly silk fibroin/tannic acid coacervates for humid and underwater wood adhesives, J. Colloid Interface Sci. 632 (2023) 151–160, https://doi.org/10.1016/j.jcis.2022.11.017.
[26] L. Wang, J. Liu, W. Zhang, D. Zhang, J. Li, S. Zhang, Biomimetic soy protein-based exterior-use films with excellent UV-blocking performance from catechol derivative Acacia mangium tannin, J. Appl. Polym. Sci. 138 (2021), https://doi.org/10.1002/app.50185.
[27] M. Podlena, M. Böhm, D. Saloni, G. Velarde, C. Salas, Tuning the adhesive properties of soy protein wood adhesives with different coadjutant polymers, nanocellulose and lignin, Polymers (Basel) 13 (2021) 1–16, https://doi.org/10.3390/polym13121972.
[28] Z. Wang, H. Kang, W. Zhang, S. Zhang, J. Li, Improvement of Interfacial Adhesion by Bio-Inspired Catechol-Functionalized soy protein with Versatile Reactivity: Preparation of fully utilizable Soy-Based Film, Polymers (Basel) 9 (2017), https://doi.org/10.3390/polym9030095.
[29] S.D. Zhou, L. Huang, L. Meng, Y.F. Lin, X. Xu, M.S. Dong, Soy protein isolate -(-)-epigallocatechin gallate conjugate: Covalent binding sites identification and IgE binding ability evaluation, Food Chem. 333 (2020), https://doi.org/10.1016/j.foodchem.2020.127400.
[30] W. Huang, X. Sun, Adhesive properties of soy proteins modified by urea and guanidine hydrochloride, JAOCS, J. Am. Oil Chem. Soc. 77 (2000) 101–104, https://doi.org/10.1007/s11746-000-0016-6.
[31] M. Villiou, J.I. Paez, A. Del Campo, Photodegradable hydrogels for cell encapsulation and tissue adhesion, ACS Appl. Mater. Interfaces 12 (2020) 37862–37872, https://doi.org/10.1021/acsami.0c08568.
[32] R. Gaglione, E. Dell'Olmo, A. Bosso, M. Chino, K. Pane, F. Ascione, F. Itri, S. Caserta, A. Amoresano, A. Lombardi, H.P. Haagsman, R. Piccoli, E. Pizzo, E.J. A. Veldhuizen, E. Notomista, A. Arciello, Novel human bioactive peptides identified in Apolipoprotein B: Evaluation of their therapeutic potential, Biochem. Pharmacol. 130 (2017) 34–50, https://doi.org/10.1016/j.bcp.2017.01.009.
[33] M. Iacomino, F. Weber, M. Gleichenhagen, V. Pistorio, L. Panzella, E. Pizzo, A. Schieber, M. D'Ischia, A. Napolitano, Stable benzacridine pigments by oxidative coupling of chlorogenic acid with amino acids and proteins: toward natural product-based green food coloring, J. Agric. Food Chem. 65 (2017) 6519–6528, https://doi.org/10.1021/acs.jafc.7b00999.
[34] J. Zhang, W. Xue, Y. Dai, L. Wu, B. Liao, W. Zeng, X. Tao, Double network hydrogel sensors with high sensitivity in large strain range, Macromol. Mater. Eng. 306 (2021), https://doi.org/10.1002/mame.202100486.
[35] J.M. Zuidema, C.J. Rivet, R.J. Gilbert, F.A. Morrison, A protocol for rheological characterization of hydrogels for tissue engineering strategies, J. Biomed. Mater. Res. - Part B Appl. Biomater. 102 (2014) 1063–1073, https://doi.org/10.1002/jbm.b.33088.
[36] T.D. O'Flynn, S.A. Hogan, D.F.M. Daly, J.A. O'Mahony, N.A. McCarthy, Rheological and solubility properties of soy protein isolate, Molecules 26 (2021), https://doi.org/10.3390/molecules26103015.
[37] M. Wang, Z. Yin, W. Sun, Q. Zhong, Y. Zhang, M. Zeng, Microalgae play a structuring role in food: Effect of spirulina platensis on the rheological, gelling characteristics, and mechanical properties of soy protein isolate hydrogel, Food Hydrocoll. 136 (2023), 108244, https://doi.org/10.1016/j.foodhyd.2022.108244.
[38] S. Shahbazizadeh, S. Naji-Tabasi, M. Shahidi-Noghabi, Development of soy protein/sodium alginate nanogel-based cress seed gum hydrogel for oral delivery of curcumin, Chem. Biol. Technol. Agric. 9 (2022) 1–12, https://doi.org/10.1186/s40538-022-00304-4.
[39] P. Persico, V. Ambrogi, A. Baroni, G. Santagata, C. Carfagna, M. Malinconico, P. Cerruti, Enhancement of poly(3-hydroxybutyrate) thermal and processing stability using a bio-waste derived additive, Int. J. Biol. Macromol. 51 (2012) 1151–1158, https://doi.org/10.1016/j.ijbiomac.2012.08.036.
[40] C.Y. Zou, X.X. Lei, J.J. Hu, Y.L. Jiang, Q.J. Li, Y.T. Song, Q.Y. Zhang, J. Li-Ling, H. Q. Xie, Multi-crosslinking hydrogels with robust bio-adhesion and pro-coagulant activity for first-aid hemostasis and infected wound healing, Bioact. Mater. 16 (2022) 388–402, https://doi.org/10.1016/j.bioactmat.2022.02.034.
[41] I. De Luca, F. Di Cristo, R. Conte, G. Peluso, P. Cerruti, A. Calarco, In-Situ thermoresponsive hydrogel containing resveratrol-loaded nanoparticles as a localized drug delivery platform for dry eye disease, Antioxidants 12 (2023), https://doi.org/10.3390/antiox12050993.
[42] S. Ghahri, X. Chen, A. Pizzi, R. Hajihassani, A.N. Papadopoulos, Natural tannins as new cross-linking materials for soy-based adhesives, Polymers (Basel) 13 (2021) 1–15, https://doi.org/10.3390/polym13040595.
[43] L.S. Kocheva, A.P. Karmanov, M.V. Mironov, V.A. Belyy, I.N. Polina, S. A. Pokryshkin, Characteristics of chemical structure of lignin biopolymer from Araucaria relict plant. Questions and answers of evolution, Int. J. Biol. Macromol. 159 (2020) 896–903, https://doi.org/10.1016/j.ijbiomac.2020.05.150.
[44] H. Kang, Z. Wang, W. Zhang, J. Li, S. Zhang, Physico-chemical properties improvement of soy protein isolate films through caffeic acid incorporation and tri-functional aziridine hybridization, Food Hydrocoll. 61 (2016) 923–932, https://doi.org/10.1016/j.foodhyd.2016.07.009.
[45] L. Panzella, G. D'Errico, G. Vitiello, M. Perfetti, M.L. Alfieri, A. Napolitano, M. D'Ischia, Disentangling structure-dependent antioxidant mechanisms in phenolic polymers by multiparametric EPR analysis, Chem. Commun. 54 (2018) 9426–9429, https://doi.org/10.1039/c8cc05989f.
[46] W.L. Boatright, M.S. Jahan, B.M. Walters, A.F. Miller, D. Cui, E.J. Hustedt, Q. Lei, Carbon-centered radicals in isolated soy proteins, J. Food Sci. 73 (2008), https://doi.org/10.1111/j.1750-3841.2008.00693.x.
[47] W.L. Boatright, L. Qingxin, M.S. Jahan, Effect of storage conditions on carbon-centered radicals in soy protein products, J. Agric. Food Chem. 57 (2009) 7969–7973, https://doi.org/10.1021/jf900087v.
[48] K. Friesen, C. Chang, M. Nickerson, Incorporation of phenolic compounds, rutin and epicatechin, into soy protein isolate films: Mechanical, barrier and cross-linking properties, Food Chem. 172 (2015) 18–23, https://doi.org/10.1016/j.foodchem.2014.08.128.
[49] H. Wang, L. Wang, Developing a bio-based packaging film from soya by-products incorporated with valonea tannin, J. Clean. Prod. 143 (2017) 624–633, https://doi.org/10.1016/j.jclepro.2016.12.064.
[50] M. Tsuruya, Y. Niwano, K. Nakamura, T. Kanno, T. Nakashima, H. Egusa, K. Sasaki, Acceleration of proliferative response of mouse fibroblasts by short-time pretreatment with polyphenols, Appl. Biochem. Biotechnol. 174 (2014) 2223–2235, https://doi.org/10.1007/s12010-014-1124-7.
[51] H.S. Song, T.W. Park, U.D. Sohn, Y.K. Shin, B.C. Choi, C.J. Kim, S.S. Sim, The effect of caffeic acid on wound healing in skin-incised mice, Korean, J. Physiol. Pharmacol. 12 (2008) 343–347, https://doi.org/10.4196/kjpp.2008.12.6.343.
[52] P.S. Kaparekar, S. Pathmanapan, S.K. Anandasadagopan, Polymeric scaffold of Gallic acid loaded chitosan nanoparticles infused with collagen-fibrin for wound dressing application, Int. J. Biol. Macromol. 165 (2020) 930–947, https://doi.org/10.1016/j.ijbiomac.2020.09.212.
[53] J. Liu, H. Yong, X. Yao, H. Hu, D. Yun, L. Xiao, Recent advances in phenolic-protein conjugates: Synthesis, characterization, biological activities and potential applications, RSC Adv. 9 (2019) 35825–35840, https://doi.org/10.1039/c9ra07808h.
[54] Z.Q. Wang, Q.Y. Song, J.C. Su, W. Tang, J.G. Song, X.J. Huang, J. An, Y.L. Li, W. C. Ye, Y. Wang, Caffeic acid oligomers from Mesona chinensis and their In Vitro antiviral activities, Fitoterapia 144 (2020), 104603, https://doi.org/10.1016/j.fitote.2020.104603.
[55] N. Varshney, A.K. Sahi, S. Poddar, S.K. Mahto, Soy protein isolate supplemented silk fibroin nanofibers for skin tissue regeneration: Fabrication and characterization, Int. J. Biol. Macromol. 160 (2020) 112–127, https://doi.org/10.1016/j.ijbiomac.2020.05.090.
[56] S. Ahn, C.O. Chantre, A.R. Gannon, J.U. Lind, P.H. Campbell, T. Grevesse, B. B. O'Connor, K.K. Parker, Soy Protein/Cellulose Nanofiber Scaffolds Mimicking Skin Extracellular Matrix for Enhanced Wound Healing, Adv. Healthc. Mater. 7 (2018) 1–13, https://doi.org/10.1002/adhm.201701175.
[57] Y. Zhao, Z. Wang, Q. Zhang, F. Chen, Z. Yue, T. Zhang, H. Deng, C. Huselstein, D. P. Anderson, P.R. Chang, Y. Li, Y. Chen, Accelerated skin wound healing by soy protein isolate–modified hydroxypropyl chitosan composite films, Int. J. Biol. Macromol. 118 (2018) 1293–1302, https://doi.org/10.1016/j.ijbiomac.2018.06.195.
[58] Q. Zong, X. Peng, Y. Ding, H. Wu, C. Lu, J. Ye, W. Sun, J. Zhang, Y. Zhai, Multifunctional hydrogel wound dressing with rapid on-demand degradation

property based on aliphatic polycarbonate and chitosan, Int. J. Biol. Macromol. 244 (2023), 125138, https://doi.org/10.1016/j.ijbiomac.2023.125138.
[59] P. Kaparekar, S.K. Anandasadagopan, In vitro and in vivo effect of novel GA-CSNPs loaded col-fibrin nanocomposite, J. Biomed. Mater. Res. - Part B Appl. Biomater. 111 (2022) 1074–1088, https://doi.org/10.1002/jbm.b.35215.
[60] C. Greene, H.T. Beaman, D. Stinfort, M. Ramezani, M.B.B. Monroe, Antimicrobial PVA hydrogels with tunable mechanical properties and antimicrobial release profiles, J. Funct. Biomater. 14 (2023), https://doi.org/10.3390/jfb14040234.